

- III) The evolution of the Cingöz Formation has to be seen in the context of the evolution of the Neogene fill of the northern Adana Basin. Revision and/or more details of the biostratigraphic and lithostratigraphic framework are necessary to gain a fuller picture of the formations' relationships. Especially with regard to the subsurface data set, the suggested presence of, for example, Karaisali reefal and Kaplankaya slope, needs to be addressed.
- IV) Geochemical provenance studies as tested in a pilot study by Satur (1999) may further help to determine i) the distal extend of W-Fan progradation and ii) help tying borehole data into the existing data set. This geochemical stratigraphy might help differentiating the various and changing sources (channel 1 - 3 and/or 3 / 4) and counteract problems arising from faulting or missing biostratigraphy.
- V) No information on climatic conditions during the Middle Miocene is presently available. Climatic data would further enhance the knowledge of possible and/or changing controls of the Cingöz Formation.

2.10 Summary

The E-Fan of the Miocene Cingöz Formation, southern Turkey, represents a small, coarse-grained multiple sourced deep-water clastic system whose evolution was fundamentally governed by tectonism and the gradually rising sea level. Initially source area uplift resulted in the initiation of the fan system and the formation of a gravel-dominated system, depositing thick coarse clastics far into the basin.

Gradual denudation of the source area in combination with rising sea level led to a sand-dominated system. Sand was deposited in coarse-grained, aggradational channel-lobe transition zones and thick lobe deposits (akin to type II and later type I ? system *sensu* Mutti 1985a), backfilling the feeder system. Basinfloor topography played a crucial role in influencing the temporal and spatial sandstone distribution pattern resulting in locally enhanced deposition, (western-) lateral restricted development and the apparent eastern deflection of the E-Fan, while basin-margin and source-area tectonism controlled the timing and activity of the source-area supply. During its final stage (early Serravallian), the E-Fan probably developed as a channel-levee complex (type III system).

The marked retrogressional signature of the E-Fan is produced by a combination of gradually rising sea level, probably subsiding source-area tectonism and denudation of the hinterland. Episodic tectonic activity resulted in influx of coarse sediment into the basin, while higher frequency sea level fluctuations resulted in occasional progradation of the deep-water system. Clastic deposition is eventually shut off and thick basinal shales blanket the Cingöz Formation.

3 CHARACTERISATION OF SUBSURFACE LOBE DEPOSITS: S10 INTERVAL, SCAPA SANDSTONE MEMBER, SCAPA FIELD, BLOCK 14/19 NORTH SEA, UK

3.1 Geological background

3.1.1 Location

The Scapa Field is located in UK Block 14/19 in the Scapa-Highlander subbasin ("Scapa syncline") of the Witch Ground Graben (WGG), Outer Moray Firth, 112 miles (~ 175 km) north east of Aberdeen in a water depth of 385 feet (120 m). The field was discovered in 1975 by appraisal well 14/19-15 (McGann *et al.* 1991) and consists of the Main Scapa Field and the West Scapa Field, divided by the West Scapa Fault (fig. 3.1).

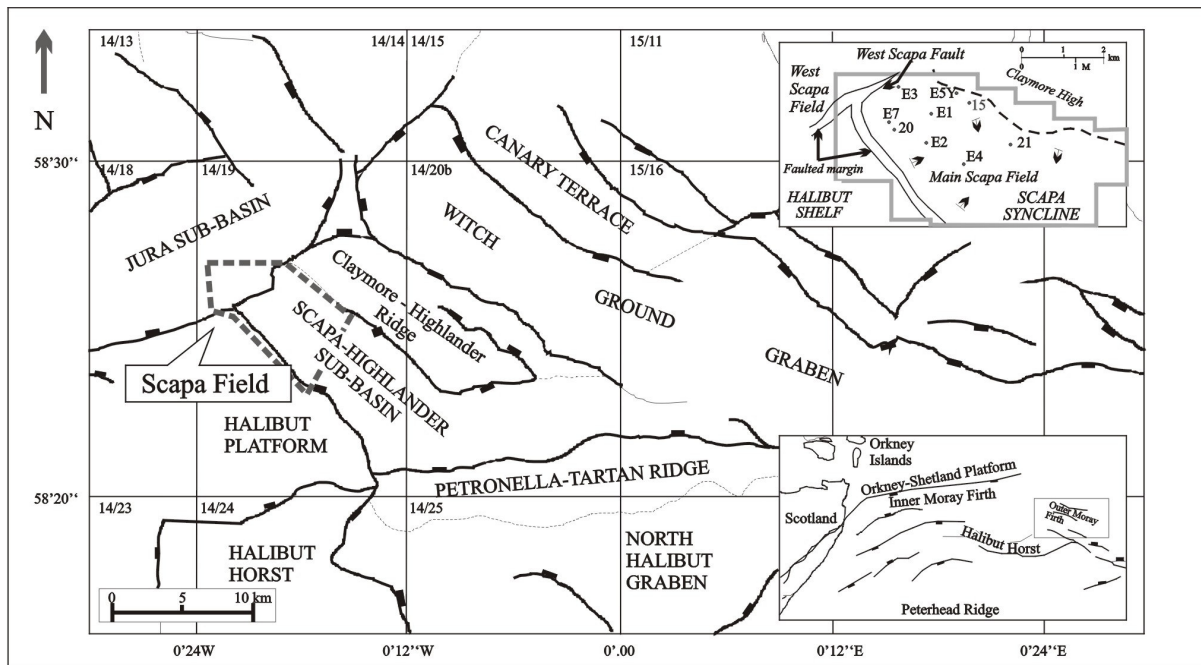


Fig 3.1: General map of the Outer Moray Firth showing the main structural elements and location of the Scapa Field. Lower inset: regional setting of the Outer Moray Firth (from McCants & Burley 1996), upper inset: elements of the Scapa Field and position of study wells.

Approximately 400 m of Early Cretaceous deep-marine sediments accumulated in the 8 x 4 km large, NW-SE trending Scapa syncline, which is located between the Halibut Shelf and Horst to the south and Claymore High to the north (fig. 3.1; Riley *et al.* 1992; Oakman & Partington 1998). The reservoir-forming sands and conglomerates of the Scapa Sandstone Member are a maximum of 586 feet (179 m) thick (Harker *et al.* 1987), forming the only other significant Early Cretaceous deep-marine play in the Central North Sea besides the Britannia field (Oakman & Partington 1998).

3.1.2 Tectono-sedimentary evolution and stratigraphy of the Scapa Syncline

In the Middle Jurassic the “Mid-Cimmerian Phase” introduced significant palaeogeographical changes in the North Sea area. The Central Graben and Viking Graben developed into major rift systems in the Late Jurassic following thermal collapse of the Jurassic Central North Sea volcanic province (Ziegler 1981). The NW-SE trending Witch Ground Graben (WGG) was initiated in the latest Jurassic forming a complex structure of submarine basins separated by intragaben highs (O’Driscoll *et al.* 1990). This process has often been related to tilt-block rotation during a long period of extension (Boote & Gustav 1987), or, more recently, to the regional transpression regime active from the Late Jurassic onwards, resulting in the syn-transpressional Scapa syncline (Oakman & Partington 1998).

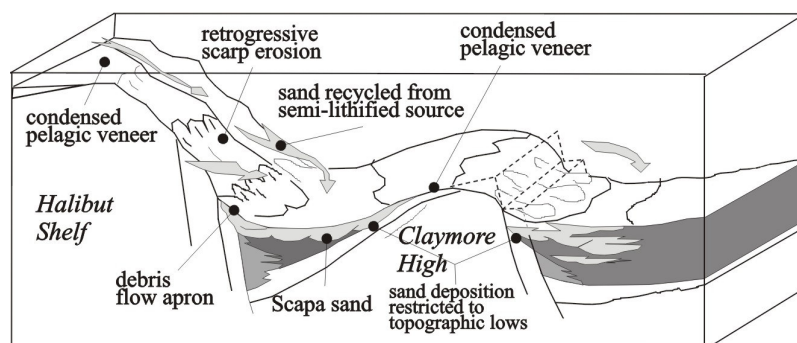


Fig 3.2: Reconstruction of the depositional environment in the Scapa-Subbasin during the Neocomian (Boote & Gustav 1987).

The rapid subsidence in late Kimmeridgian - early Volgian times produced a deep basin with graben collapse in late Volgian times (Late Cimmerian tectonism). During this period, the entire graben and surrounding platform were blanketed by Volgian - early Ryazanian black shales (**Kimmeridge Clay Formation**; Boote & Gustav 1987). A major phase of regional subsidence in

the Ryazanian introduced oxygenated conditions leading to the deposition of calcareous shales and coccolithic marls as lowest part of the transgressive **Valhall Formation** (Harker *et al.* 1987). Renewed Cimmerian tectonic activity resulted in emergence of the Halibut Horst, Claymore High and Tartan Ridge (O’Driscoll *et al.* 1990; Oakman & Partington 1998). During the late Ryazanian - late Valanginian large volumes of conglomeratic facies were deposited in the regions adjacent to the Halibut Shelf (fig. 3.2). Much of the material is interpreted to be Carboniferous, sourced directly from the fault scarp (Boote & Gustav 1987). Waning tectonism and gradual eustatic sea-level rise (Haq *et al.* 1987a,b) resulted in reduced conglomeratic input and the accumulation of sand-grade material on the Halibut Shelf. This material was subsequently redeposited as sand-rich turbidites across the Scapa syncline (O’Driscoll *et al.* 1990), forming the **Scapa Sandstone Member** of the Valhall Formation (early Valanginian – late Hauterivian) (figs. 3.2, 3.3; Harker *et al.* 1987). In the early Barremian, clastic sedimentation was cut off as sea level rose, ending sand deposition in the Scapa syncline (Harker *et al.* 1987; Riley *et al.* 1992). Marls and limestones of the Upper Valhall Formation blanketed the area, succeeded by Aptian-Albian shales and marls (**Sola and Rodby Formations**) and thick Late Cretaceous pelagic marls, limestones and biogenic carbonates (**Chalk Group**, fig. 3.3; Harker *et al.* 1987). Tertiary structural inversion was restricted to the Inner Moray Firth while a thick shallowing-up sequence of submarine fan to shallow marine/paralic sands was deposited over the Outer Moray Firth as gradual down-warping continued through the Tertiary and Quaternary. Little tectonic activity has occurred since (Hendry 1994).

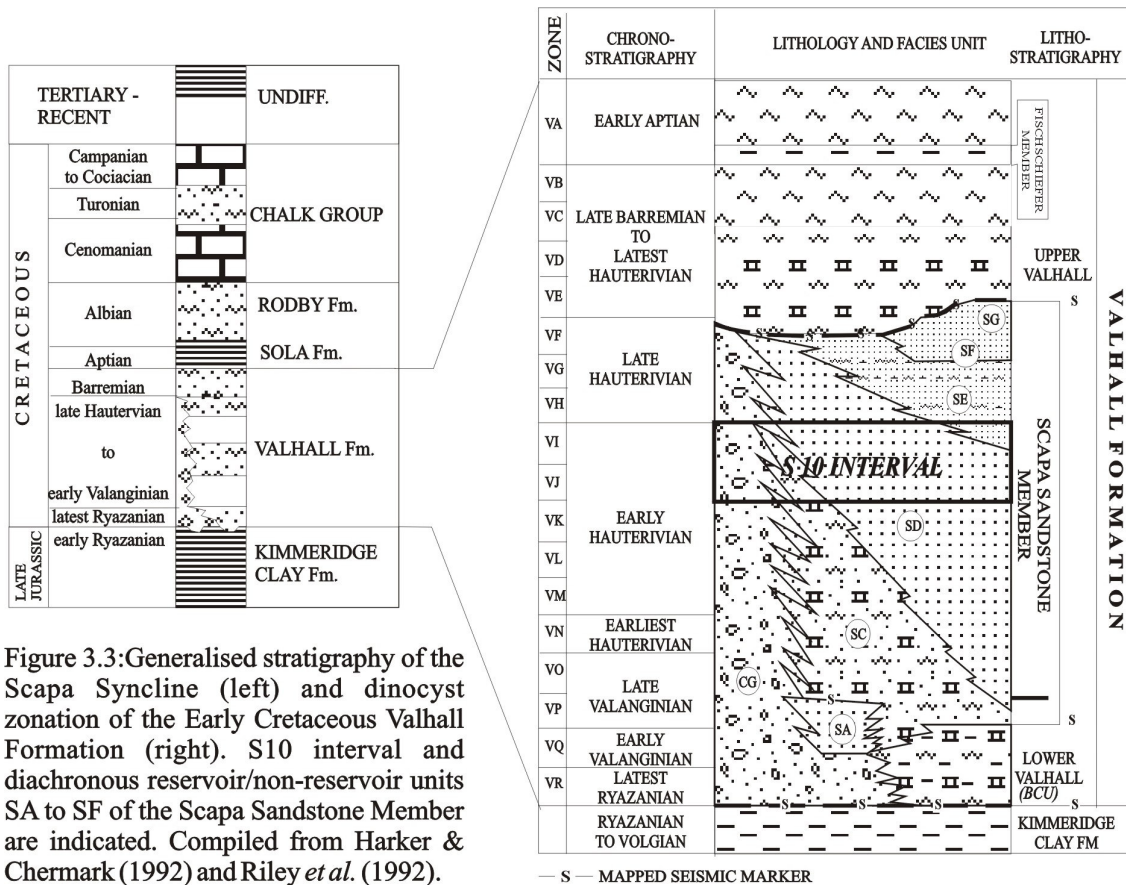


Figure 3.3: Generalised stratigraphy of the Scapa Syncline (left) and dinocyst zonation of the Early Cretaceous Valhall Formation (right). S10 interval and diachronous reservoir/non-reservoir units SA to SF of the Scapa Sandstone Member are indicated. Compiled from Harker & Chermak (1992) and Riley *et al.* (1992).

The current SE-plunging synclinal geometry of the Scapa Field is due to differential compaction resulting from increased loading during the Late Cretaceous and Tertiary when the Early Cretaceous conglomerates close to the Halibut Platform compacted to a lesser degree than the laterally equivalent marls and sands (McGann *et al.* 1991). Generally, very little faulting is present, except for the major faults that mark the southern limit of the field (fig. 3.4, McGann *et al.* 1991).

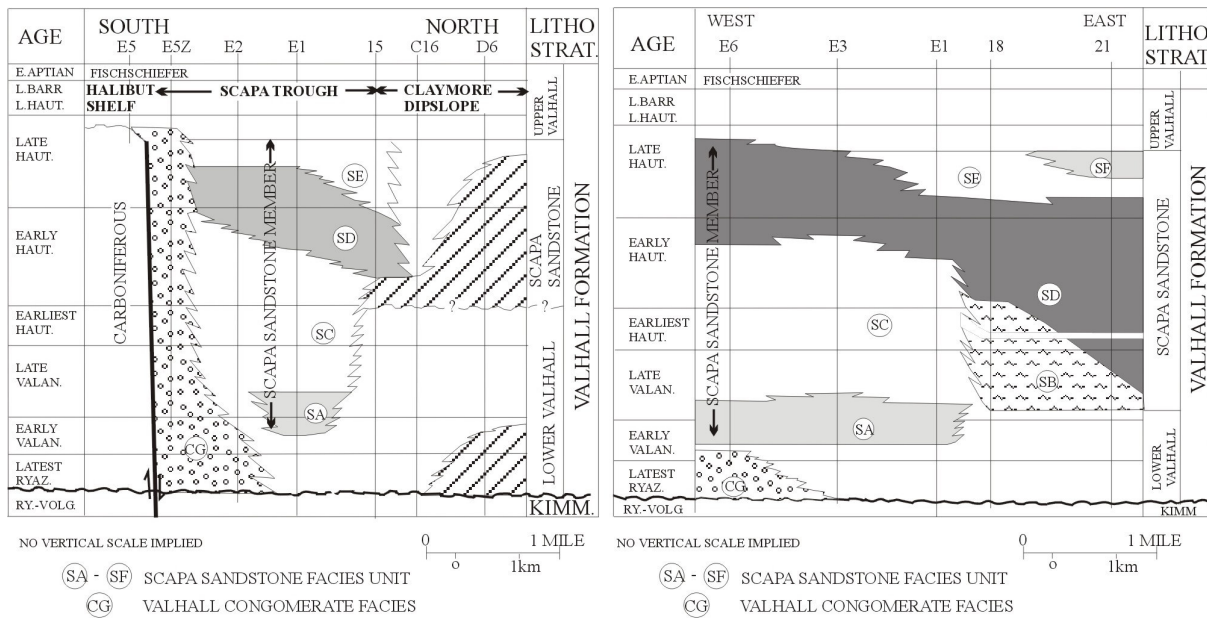


Figure 3.4: Schematic Scapa Field dip and strike stratigraphic sections showing complex relationships of reservoir and non-reservoir unit facies (from Riley *et al.* 1992).

3.1.3 The Scapa Sandstone Member

The Scapa Sandstone Member (SSM) forms part of the transgressive Valhall Formation (Harker *et al.* 1987). The Valhall Formation has a maximum stratigraphic extent from latest Ryazanian - Early Aptian which Riley *et al.* (1992) subdivided into 18 palynological zones principally based on dinocyst distribution, relative abundance and palynomorph associations (fig. 3.3). The SSM is dated Early Valangian (134 myr) to intra-late Hauterivian (126 myr; fig. 3.3; zones VG to VR in descending order). During this period, a maximum of 586 feet (179 m) of turbiditic sandstones, conglomerates and marls were deposited in a marine setting with water depth in the order of 500 ft (152 m) before rising sea level effectively ended clastic deposition (O’Driscoll *et al.* 1990; Riley *et al.* 1992).

Marked lateral and vertical lithological variations are present within the SSM. Laterally, a distinct bimodal distribution of facies can be observed with a conglomerate fringe (CG) close to the faulted margin of the Halibut Shelf while turbiditic sandstones, marls and limestone are deposited in the Scapa syncline (fig. 3.4). Vertically, the SSM is traditionally divided into several units: SA to SF. The thinly bedded, fine to medium-grained turbidite sands of units SA, SD, and SF form the reservoir units, while units SB, SC and SE are dominantly composed of tight sandstones, marls and muddy sandstones (fig. 3.4; McGann *et al.* 1991). These units are largely diachronous and their distribution is spatially and temporally restricted (Riley *et al.* 1992). Environmental and developmental reconstructions of the Scapa turbidite system are based on these diachronous units (e.g. Harker *et al.* 1991; McAfee 1993; Hendry 1994), however, Riley *et al.* (1992) present the dinocyst-based chronostratigraphic evolutionary model for the first time (fig. 3.5).

Initially, sand deposition (SA) only took place in the NW of the field (fig. 3.5a) while lower Valhall marls and limestones were deposited in the Scapa syncline (zone VP / late Valangian). Tightly cemented sandstones and limestones (unit SB) were deposited in the east (fig. 3.4) while unit SC marls, limestones and conglomerates cap unit SA in the northwest of Scapa (late Valangian - early Hauterivian). Unit SC is time-equivalent to units SA, SD and SE (fig. 3.4). In the Early Hauterivian (zone VM to VL) deposition of unit SD began in the southeast of the field (fig. 3.5b) and commenced during the early - late Hauterivian (zones VI/VJ) by which time the SD sand deposition covered most of the Scapa syncline (fig. 3.5c). Deposition during the SD took place as series of offset stacked, detached sand lobes and basinfloor fans (McAfee 1993). During the later Hauterivian, SD sand deposition continued in the northwest. Marls and tight sandstones of unit SE capped SD deposition in the central area (zone VG-VH) while a separate sandy fan system (SF) developed in the southeast (fig. 3.5d; zone VG). Throughout the deposition of the SSM, conglomerates were shed off and deposited along the faulted shelf margin. Clastic supply was cut off by

Late Hauterivian (dated as intra-zone VG) as the sea-level rose (Riley *et al.* 1992). Marls and limestones of the upper Valhall then blanketed the entire area (Harker *et al.* 1991).

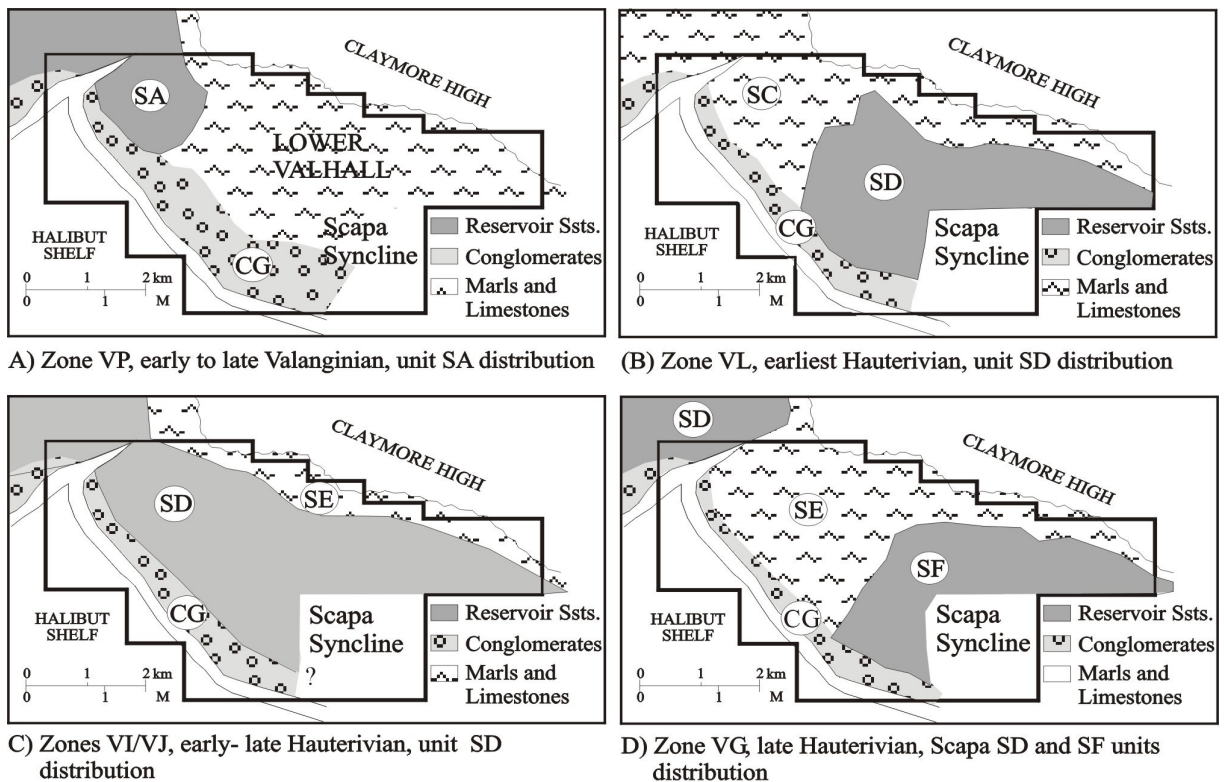


Fig 3.5: Distribution of reservoir / non-reservoir units of the Scapa Sandstone Member in the Main Scapa Field (from Riley *et al.* 1992).

The Scapa turbidite system is mineralogically relatively immature (Green 1990). The sandstone composition broadly ranges from fossiliferous quartz arenites to subarkoses and sublithoarkoses (Hendry 1994). Fossiliferous components include penecontemporaneous Valhall, Jurassic and older Late Palaeozoic taxa. Carboniferous reworking is particularly prominent in the conglomerate facies fringing the Halibut Shelf (e.g. Boote & Gustav 1987; Harker & Chermak 1992; Riley *et al.* 1992), while Late Jurassic and/or Neocomian reworking predominated in more distal locations (Riley *et al.* 1992). The abundance of stenohaline, bioclastic material throughout suggests that sands were reworked from a nearby shallow marine high-energy, high-productivity environment believed to be the Halibut Shelf (Hendry 1994). Occasional polymict shale-matrix conglomerate within unit SD are interpreted to reflect sporadic tectonism where material is derived directly from the fault scarp (Hendry 1994). Background sedimentation includes hemipelagic shales and marls and tuffs, the latter preserved as green shales (Harker & Chermak 1992; Hendry 1994).

Sediments entered the basin through persistent, preferred feeder zones along the Halibut Shelf, probably along structural lineaments (McAfee 1993). The focus of the sand deposition is known to have moved (fig. 3.5) (Riley *et al.* 1992), which is explained by antecedent lobe topography having influenced the path of successive flows. The SSM was deposited during a time of general eustatic sea level rise (Haq *et al.* 1987a,b; Harker *et al.* 1991) and the uplift history of the shelf may have influenced its facies distributions and thereby the nature of material reworked into the basin. Sand-poor non-reservoir intervals probably reflect temporary deepening of the clastic source area (shelf) and increased hemipelagite deposition (Hendry 1994). The narrow width of the Scapa syncline probably favoured axial deflection of the turbiditic flows by the steep ramp formed on the SE-flank of the Claymore High in the north (Oakman & Partington 1998).

The apparent lack of internal organisation suggests deposition analogue to a slope apron (McAfee 1993) or a submarine ramp environment (Hendry 1994) where the deposition of sediments is believed to take place in broad, shallow sandy channels and subordinate lobes (Boote & Gustav 1987; McAfee 1993).

3.2 The S10 Interval

Elf Occidental Caledonia Ltd reorganised the SSM into chronostratigraphic intervals ranging from S1 (lowerst) to S13 (uppermost) based on Riley's *et al.* (1992) dinocyst stratigraphy. The S10 interval comprises the late Early Hauterivian palynological zones VI and VJ (fig. 3.3, 3.6). It contains most of the oil-bearing unit SD as well as parts of the non-reservoir unit SE and the conglomeratic CG facies. Abundant lithological analysis, sedimentological and petrophysical data exist for unit SD (e.g. Harker & Chermak 1992; McAfee 1993; Hendry 1994), however, no detailed environmental and developmental analysis for the chronostratigraphic S10 interval and its (sub-) zones has been undertaken.

Chronostratigraphic interval	Dinocyst zone	Zone top datum	Dinocyst subzone	Subzone top datum
S 10	upper	Lithodina pertusa		
	lower	downsection increase of <i>Gonyaulacysta cladophora</i> Duxbury and <i>Cassiculosphaeridia magna</i>	VJ1	[not further described]
			VJ2	downsection increase <i>Athigmatocysta glabra</i>
			VJ3	localised downsection incr. <i>Oligosphaeridium sp.</i>

Figure 3.6: Dinocyst zones comprised in the S10 interval of the Scapa Sandstone Member (from Riley *et al.* 1992).

3.2.1 S10 framework

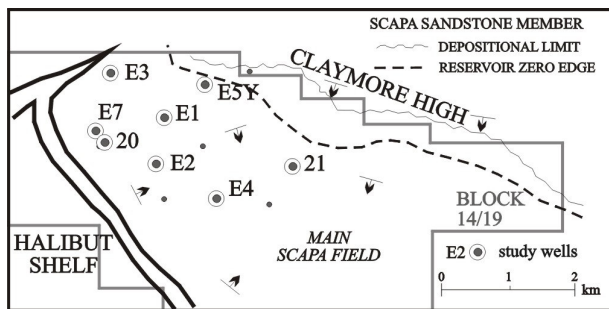


Figure 3.7: Location of study wells within the Scapa Main Field (after McGann *et al.* 1991).

The aim of this study is to characterise the non-channelized sandy turbidite facies (lobe deposits) and the controls governing their accumulation in the light of the spatial and temporal development of the S10 interval.

Previous studies focused on the diachronous SD unit and its subunits, thus a working S10 framework had to be established. Lithofacies analysis integrated with petrophysical data of 8 wells with proven S10 interval presence form the basic framework (fig. 3.7; table 3.1), supported by data compiled from published and unpublished reports. The study included:

- core logging of 785 feet TST (238 m) of S10 interval and undifferentiated SD/SC/SE which are presumed to be part of the S10 interval (enclosure 1)
- establishment of a refined lithofacies scheme to grasp subtle lithological variations (*chapter 3.2.1*)
- integration of petrophysical data for lithofacies reconstruction of uncored S10 interval (*chapter 3.2.1*)
- interwell correlation (*chapter 3.2.2*)
- definition of fan depositional environments *sensu* Mutti & Normark (1987, 1991) (*chapter 3.3*)
- analysis of spatial and temporal development of sandstone bodies and assemblages, establishing depositional model and controls of S10 interval and its (sub-) zones (*chapter 3.4*)

	14/19-20	14/19-21	14/19-E1	14/19-E2	14/19-E3	14/19-E4	14/19-E5Y	14/19-E7
S10 - total	176	47.5	193	nd (193-176?)	113	131	236	nd (176-113?)
VI	37	absent	32.5	nd (32.5-37?)	55	67	absent	nd (>37-<55?)
VJ - total	139	47.5	160.5	nd (160.5-139?)	58	64	236	nd (139-58 (100?))
VJ1	absent	4.5	49	nd (49 - > 0)	nd	nd	178	nd (absent?)
VJ2	48.4	25	40.4	nd (40.4-48.4?)	nd	nd	34	nd (<48.4)
VJ3	90.6	18	71	nd (71-92?)	nd	nd	24	nd(<92)

All thicknesses in feet TST.

Table 3.1: Thicknesses of S10 zones and subzones in study wells. Note that not always sharp boundaries exist between zones, presumably due to sampling range and quality. In these cases the maximal extend was often chosen as „true“ zone thickness and/or if bases/tops correspond to marked changes in wireline response. nd = non-differentiated, () = estimates based on neighbouring wells.

Lithofacies analysis

A lithofacies scheme to accommodate subtle facies variations was introduced. It is based on the grain size of the dominant components resulting in six lithofacies groups: **Gravel**, **Gravel-Sand**, **Sand**, **Sand-Mud**, **Shale** and **Biogenic** facies (fig. 3.8; plates 7 - 8). Further subdivisions are based on sedimentary structures and dominant clast lithologies leading to a total of 20 lithofacies types. Measured helium porosity and air permeability values are given for the different lithofacies types where available (data from McAfee 1993). The cored S10 interval is dominated by deposits of the S (58.7 %) and GS facies (25.5 %) (fig. 3.9). Less common are sediments of the G (8.6 %) and SM facies (5.6 %), while marls (BI facies: 1.2%) and SH deposits (0.2 %) are rare. Wells E1, E2, E5Y and E7 (west-central-north position) are characterised by gravel facies and an above average amount of sand facies (fig. 3.9; enclosure 1), while wells 20, 21, and E4 (proximal central-southern position) are dominated by S facies (20, 21; plate 8.2/3) and higher amounts of SM facies (E4, 21; plate 8.4-6). GS and G facies deposits (20, 21; plate 7) are rare.

Electrofacies analysis

a) Lithofacies reconstruction

The integration of petrophysical data became necessary to broadly interpret lithologies and changes in lithology of the uncored S10 interval. In a first step, the differentiated lithofacies group and types were calibrated against the wireline logs resulting in broadly recognisable petrophysical signatures for the various groups (table 3.2). Generally, shales appear to be the most easily recognisable lithology, characterised by high gamma-ray values and a clear negative separation of the density and neutron log. Shale-clast rich G

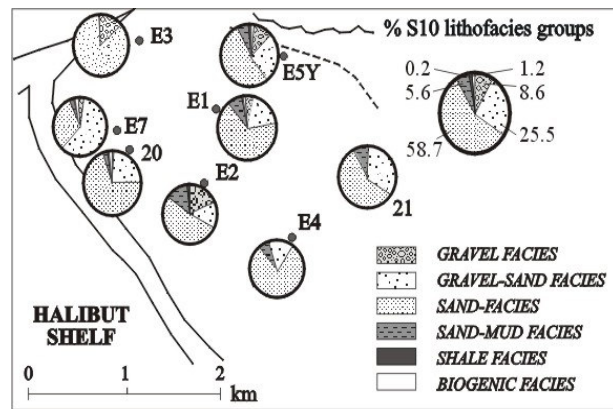


Figure 3.9: S10 Lithofacies group distribution in Main Scapa Area

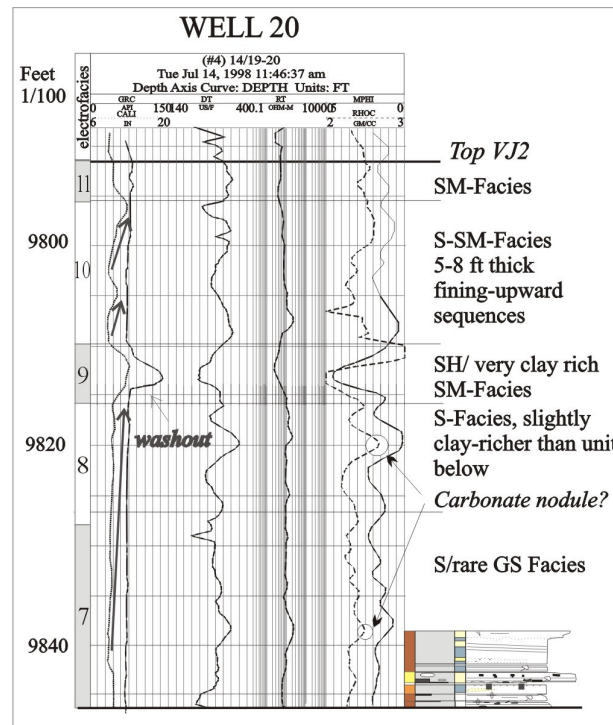
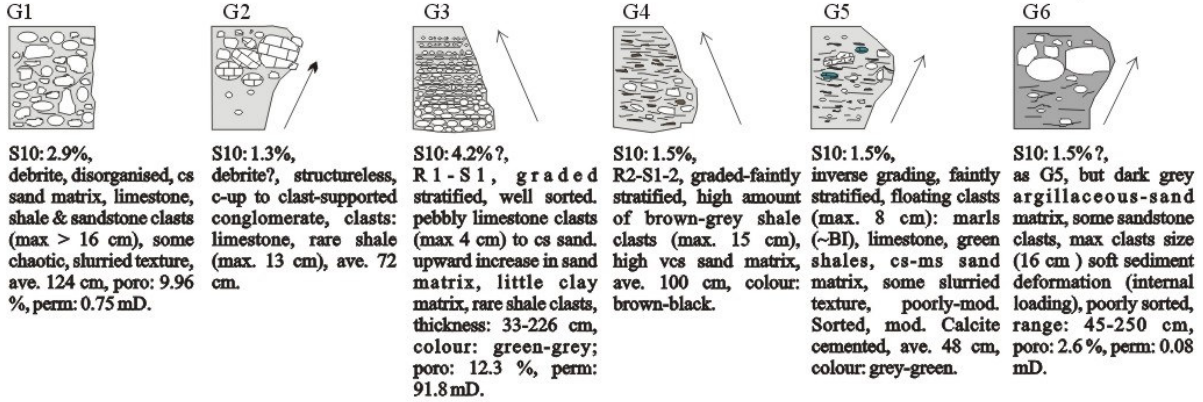
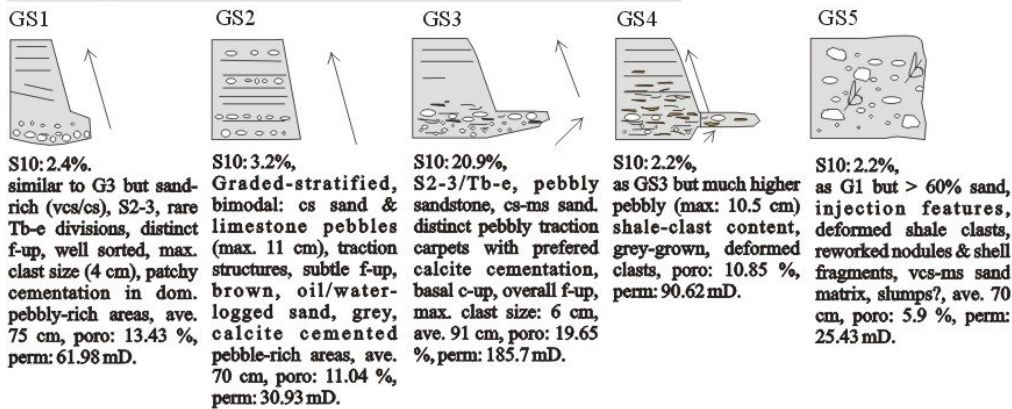


Figure 3.10: Example of lithofacies reconstruction by wireline analysis. See enclosure 1 for further lithofacies reconstruction and legend.

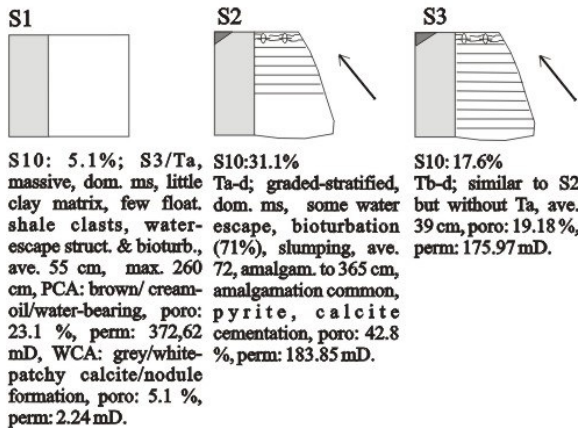
GRAVEL -Facies: gravel > 75%, sand < 25%



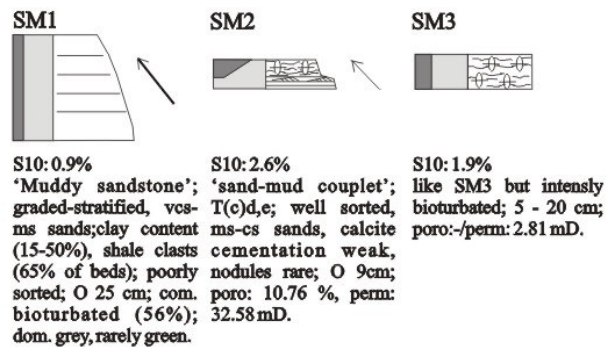
GRAVEL - SAND Facies: gravel < 25%, sand > 75%



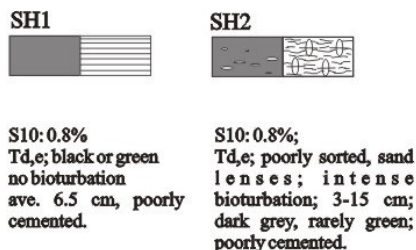
SAND-Facies: gravel < 2%, clay < 15%



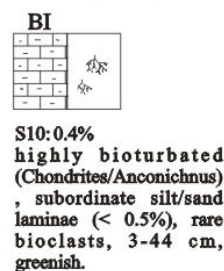
SAND - MUD Facies: sand < 75%, clay > 15%



SHALE Facies: clay and silt grade, sand < 5%



Hemipelagic marls



Legende

- vfs- very fine sand
- fs - fine sand
- ms - medium sand
- cs - coarse sand
- vcs - very coarse sand
- shale content
- sand content
- WCA: well cemented area
- PCA: poorly cemented area
- ⊕ ⊗ ⊛ bioturbation
- ⊂ shell fragments
- ↗ fining-upward
- ↘ coarsening-upward

Figure 3.8: Lithofacies classification scheme for the S10 interval. Poro-perm data from McAfee (1993).

and GS facies, for example, show slightly different wireline values than the remainder (table 3.2). The gamma-ray log is thus frequently used as shale content indicator (Rider 1996). Calcite in form of cement, nodules (both diagenetic) or as reworked limestone clasts and diagenetic pyrite* may strongly modify density readings (fig. 3.10; enclosure 1), the same applies to sedimentary structures, e.g. massive versus laminated sandstones (e.g. sonic log values: 60 vs 80, E2: 9130-45 ft), or oil/gas/water content (Rider 1996). The uncored intervals above and/or below the cored section appear to be dominated by shale-rich deposits of the SM and SH facies, interbedded with shale-rich S facies and sometimes clean S and rare GS facies deposits (enclosure 1). Marls (BI facies) are equally rare in the wireline record (e.g. E4, E5Y).

Lithofacies Group	Calliper CL in inch	Gamma-ray GR in API	Sonic log ΔL in ν s/ft	Resistivity log RT in Ohm	Density log DL in g/cm^3	Neutron log NL in NPHI	Reference in ft log depth
G	norm	25 – 35 ave 30 shale clast-rich G5/G6: - 45	60 - 70	20 – 200 peaks 500 ave 120 shale clasts (G5) or matrix (G6) lower values	2.4 – 2.65 depending on degree of cementation / nodule form. / limestone clasts	0.05 – 0.15	e.g. E5Y: 9420 E5Y: 9450 E2: 9112-25
GS	norm	20 - 35, ave 30 shale clast-rich GS4: - 50	55 – 80	80 – 300 ave 100 peaks 500	2.5 – 2.6 pebbly limestones of GS3: 2.75	0.05 – 0.15 peaks 0.2	e.g. 21: 10604 E3: 10631 – 40 (pyrite) E5Y: 9428 – 44
S	norm	30 – 45 ave 35 high shale matrix: 45 - 60	65 – 90 ave varies for diff. Trend lines	70 – 200 peaks 400 ave 120	2.2 – 2.5 depending on degree of cementation / clasts / diagen. pyrite	0.15 – 0.25 erratic trends	e.g. E1: 9070 – 5 (pyrite) E2: 9087 (pyr.) E4: 9692 E4: 9658 - 80 E5Y: 9310 - 35
SM	norm / caving / wash-out	60 - 80	60 – 80	20 – 40 peaks: 100	2.3 – 2.55 depending on degree of cementation	0.1 – 0.2 occasional negative NL/DI separation: 0.45 peak	e.g. E1: 9208 - 13 E2 : 9070 - 80 E4: 9688
SH*	caving / Wash-out	up to 135	60 (low transit times)	60	2.5	0.1 occasional negative NL/DI separation: 0.4 peak	e.g. 20 : 9765 E2: 9148 E7: 9773
BI*	norm / little caving	30 - 65	70 - 80	20 – 40 peaks: 90 - 100	2.4-2.65	0.1 – 0.15	e.g. E5Y: 9496 E7: 9893

Table 3.2: Wireline readings of lithofacies groups (norm = normal, ave = average, max = maximum). Note that some values, i.e. sonic and neutron log values are usually higher for sands and coarser sediments and lower for shale-rich sediments, marls typically show a slight negative DL/NL separation (Rider 1996). The respective thicknesses of lithofacies groups BI, SH and often SM are mostly below resolution thickness (0.6 m) thus given values are approximations.

*density: pyrite = 4.8-5.17 g/cm^3 , carbonate = 2.66-2.74 g/cm^3 , organic matter = 1.2 g/cm^3 (Rider 1996)

b) Electrosequence analysis

Electrosequence analysis^{*} *sensu* Rider (1996) is used to identify recognisable and correlatable intervals within the cored and uncored successions of the S10 interval. Trend lines (> 1 m [bed scale], 10s m [sequences] or 100s [large structures of basin filling]) record a persistent change in log value of various tool measurements while baselines (10 - >100s m = electrosequence) reflect a constant value. The latter is typically used to characterise formations.

Lithologically, the S10 interval is similar to the under- and overlying intervals. The little overall thickness and small-scale internal lithology changes necessitate a detailed analysis of the wireline records, i.e. trend line analysis *sensu* Rider (1996; fig. 3.10; enclosure 1). Appendix 2 lists the differentiated trend lines with their characteristic average log values for the S10 interval and the undifferentiated SD unit of wells E2 and E7. Trend lines are of extremely variable thickness (3 - 27 ft, e.g. E5), their bases and tops characterised by distinct breaks in wireline response of one or more tool records (e.g. well E4). The trend lines often coincide with lithological sequences or groups of sequences (*chapter 3.3*), picking up distinct as well as subtle lithology variations (e.g. E5Y: S-SH [TL 12]; 20: S/GS-S/GS-S [TL 4/5/6]). Changing log values, e.g. gamma-ray recording shaling-upward (i.e. fining-upward: bell-shaped) or shaling-downward sequences (i.e. coarsening-upward: funnel-shaped), may comprise 1 or more trend lines (e.g. shale-up: E2: srS-SM [TL 11]; E3: srS-SM-SH [TL 2]/ shale-down: E3: SH-SM-srS [TL 1], E4: SH-SM-srS [6/7]; *chapter 3.3*), while blocky patterns record alternating sand-dominated/shale-dominated intervals (e.g. well 20: sand-dom. TL top 3-6; shale-dom. TL 1/2/base 3 and 7-9]. The number of trend lines identified for the different wells is largely a function of the overall thickness and lithological heterogeneity.

3.2.2 Interwell correlation

1. Biostratigraphy: the S10 interval comprises 2 dinocyst zones and subzones (VJ1-3/VI) and is present in all 8 study wells. However, subzone resolution and total extend are not known for all the study wells (table 3.1; enclosure 1).
2. Lithology-based correlations were only possible between wells E2 and E7 where the unique G6/G3 sequence occurs in both wells (plate 7; enclosure 1). A decrease in thickness (G6/G3) and grain size (G3) from wells E2 to E7 implies a more proximal position for E2 with respect to this facies association.

For well E2, the top of the S10 interval is located between 9040-9019 ft log depth, while no biostratigraphic subdivisions at all exist for well E7. Neighbouring wells E1 (0.7 km to N) and 20 (0.8 km to W; fig. 3.7) possess 193 and 176 ft TST respectively. Thus the S10 interval of well E2 may range between 176 - 193 ft TST (table 3.1). Depending on the actual thickness and top taken, the lowest S10 base may be at 9233 ft log depth and highest base at 9186 ft log depth [9040 ft log depth + 193 /176 ft = 9233 /9216 ft log depth and 9019 ft log depth + 193/176 ft = 9203/9186 ft log depth]. These estimates place the total cored section of well E2 within the S10 interval (enclosure 1) which corresponds to Riley *et al.* (1992) diagrammatic representation which approximately correlates the base of VJ with the base of unit SD, while the top is located within unit SE.

The unique lithofacies assemblage G6/G3 in well E2 is believed to be contained within zone VJ, based on i) stratigraphic considerations (proximity to the base of the sequence) and ii) great overall VJ thicknesses in the wells E1 and 20. Well E7 contains the same distinctive lithofacies assemblage and it is therefore suggested, that the top of the cored well E7 represents zone VJ (enclosure 1). The total S10 thickness in well E7 may range between 176 and 113 ft as recorded in the adjacent wells 20 (0.25 km to SSE) and well E3 (~ 0.85 km to NNE; fig. 3.7). The proximity to well 20 suggests that presence and thicknesses of subzones might be fairly similar (table 3.1). Base and top of the S10 interval in well E7 are difficult to define, however a good part (>50 ft ?) of the uncored SE non-reservoir unit are believed to belong to the S10 interval.

* "Electrosequence: an interval defined on wireline logs, through which there are consistent or consistently changing log responses and characteristics, sufficiently distinctive to separate it from other electrosequences." (Rider 1996).

3.3 Fan environments

3.3.1 Distributary channels

Bifurcation of a system's main feeder(s) result in a network of distributary channels funnelling sediment into the basin. They are known from modern and ancient deep-water clastic system (e.g. Navy Fan: Normark *et al.* 1979; Crati Fan (Ricci Lucchi *et al.* 1985; Mississippi Fan: Schwab *et al.* 1996; Agadir turbidite system: Ericella *et al.* 1998; Paola Basin systems (Trincardi *et al.* 1995); Cingöz Formation: *chapter 2*). The S10 distributary channel-fill deposits form discrete 1 – 6 m thick, gravel-rich successions with erosional bases, often sharp tops and display either abrupt (CH 1) or gradual (CH 2) fining-upward (fig. 3.11). These channels were probably between 80 – 500 m wide, based on average width/depth ratios for mid- and lower fan channels compiled from modern and ancient submarine fan systems (Clark & Pickering 1996), however, much smaller distributary channels (~20 m width) were recorded in the proximal lobe zone of the Cingöz Formation, E-Turkey (*chapter 2.4.2*).

a) Channel-fill 1 (braided*?)

1 to 3 m thick G/GS – SM/SH associations characterise CH 1 fills (e.g. E2: G6-G3-SH; plate 7.1) which form 4.3 % of the S10. The 0.4 - 2.0 m thick G/GS abruptly fine to 0.1 – 0.3 m thick SM/SH facies (blocky grain size curve), typically involving 2 - 4 beds (fig. 3.11). Internally, sharp contacts prevail, loading is occasionally present (e.g. E2: G3 onto G6 at 9116 ft). The upward increase in shale content is reflected by increasing GR and decreasing DL / RT values and partial borehole enlargement (E5Y: 9455 - 9448 ft).

The abrupt change in lithofacies from coarse gravel deposits resulting from highly energetic processes (gravely / gravel-sandy debris flows / sandy high-density turbidites) to very fine grained, mud-rich deposits indicating a tranquil depositional environment (low density turbidites; Tc-e) suggests a sudden deactivation of the channel as a conduit. The thick debrites and succeeding gravely-sandy high density flows probably plugged the channel forcing it to avulse (Pickering *et al.* 1995; Clark & Pickering 1996). The residual topography was then infilled by silts and muds. Anderton (1995) relates rapid changes in channel location to highly unstable areas within a fan system. The observed random facies arrangement (coarse facies) is characteristic of braided channel of broad sheet-like geometries (Wüllner & James 1989), this can, however, not be confirmed for the CH 1 deposits.

The unique G6/G3 association of wells E2 and E7 shows a marked decrease in grain size (E2: 16 to E7: 6) and dramatic thinning over ~ 1 km distance (E2: 2.50 m to E7: 0.45 m). The absence of this unique facies association in well 20 (~ 0.25 km SE of E7) underlines the linear, confined nature of these deposits most likely of channel geometry (fig. 3.11). A fault-scarp source is suggested for the polymict G6 facies, triggered by sporadic tectonism (Hendry 1994).

CH 1 elements are rare, forming shallow, isolated features in the central wells E5Y/E1 and proximal wells E2/E7 (fig. 3.12).

b) Channel-fill 2 (meandering?)

CH 2 infill sequences typically involve > 4 beds of 0.1 to > 2 m thick G/GS gradually fining-upward into finer-grained, 0.1 – 0.4 m thick S/SM facies (e.g. 21: (G)-GS-S-SM [10586 - 10569 ft]; fig. 3.11). The fining-upward is accompanied by a steady decrease of the sand/shale ratio, DL and RT values, while GR and NL gradual increase. However, occasionally a shaling-down accompanies the fining-upward trend (e.g. E1: 9210-9216 ft: GS4-S2) where a shale clast-rich basal GS facies fines upward into clean sandstones. The rip-up clasts and texture of GS4 may result from short transport distances following channel margin collapse (Clark & Pickering 1996; Johansson & Stow 1995).

Generally, the more gradual and orderly fining-upward of facies involving a greater number of beds indicates longer-lived conduits which are gradually migrating across the fan surface (e.g. Einsele *et al.* 1994; Pickering *et al.* 1995; Clark & Pickering 1996) which is typical of meandering channels (Anderton 1995). Their pod-like nature resulting in considerably varying sandbody thickness down the axis of the fairway

* Typically terminology derived from fluvial systems is applied to submarine fan channels such as braided, meandering, sinuous and straight (e.g. Hein & Walker 1982, Wüllner & James 1989), Clark & Pickering (1996), however, strongly doubt the unequivocal application of planform geometries to ancient outcrops.

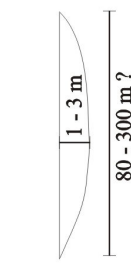
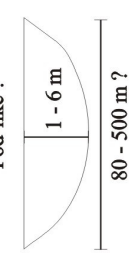
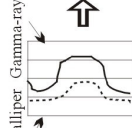
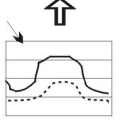
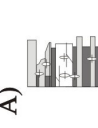

ENVIRONMENTS	SEDIMENTARY FACIES	WIRELINE RESPONSE	FACIES	ASSOCIATIONS/STACKING	GEOMETRY
CHANNEL-FILL CH I conglomerate-rich / abrupt fining-up 4.3 %	G/GS sharply topped by SM/SH facies erosive base, crude fining, 2 - 4 beds, med - thick bedded	upward + GR, occ. blocky, RT & NL decrease, DL variable	SH/SM G-Facies debris flows	lobes, CH II, OB isolated	 1 - 3 m 80 - 300 m ?
	CH II sand-rich / gradual fining-up 9 %	G/GS facies fining-upward to S/SM/SH- facies, upward increasing shale content, erosive bases, transitional and/or sharp top, Med. - thick-bedded, > 4 beds	SM- S-Facies G-GS Facies	lobe, CH I, OB isolated, stacked with CH I	Pod-like ?  1 - 6 m 80 - 500 m ?
LOBE non-channelised sandy deposits 47 %	ms - cs S1-3, subordinate GS/SM, some GS dominated, sand/shale ratio: 9:1, med. - thick-bedded, small fining-ups forming crude large coarsening- and/or fining-ups little bioturbation	GR: 20-30, SL (60- 70), low RT (20- 100), variable DL & NL	S- rare GS-Facies S-rare SM-Facies	CH I/II (erosive contact), lobe fringe, rare interlobe (mostly transitional contacts) isolated, some stacking	2.5 - 8 m sheet-like / lobate
LOBE FRINGE 28 %	fine S2-3 and SM, rare GS facies, sand/shale: 4:1, distally increasing shale content, med. - thin-bedded, dm-scale fining-up forming larger, crude coarsening- and/or fining-ups, highly bioturbated	mostly upward decreasing GR: 30- 50 API, low RT, variable DL & NL	S-Facies S-SM-Facies	lobe, OB (proximal), fan fringe/ basin plain (distal) isolated or stacked (distal)	wedge-shaped 1 - 6 m
OVERBANK/ INTERLOBE 3.5 %	thin-bedded, shale-rich SH and SM facies, low sand/shale ratio (<1:1) differentiation based on environmental association	GR: -70 API, borehole enlargement, DL/NL negative separation	SH/ SM 	A) lobe (transitional contacts), CH B) lobe, lobe fringe (both transitional contacts) A/B isolated	A) 0.5 - 1.5 m wedge-shaped B) 0.5 - 1.5 m shallow infill-geometry
FAN FRINGE / BASIN PLAIN 9 %	thin-bedded SH and very shale-rich SM facies higher shale content than OB/interlobe deposits part of larger coarsening-up units hemipelagic intercalations = basin plain	GR: 70-135 API, borehole enlargement, DL/NL negative separation	SH/ SM 	shale-rich distal lobe fringe (transitional), some hemipelagites (sharp) isolated	1 - 5 m sheet-like
HEMPELAGITES 1.2 %	strongly bioturbated marls, rare 1-3 mm silt - fine sand laminae, sharp bases and tops. associations: a) SM3-Bi-SM3 (distal/prox.); b) S2-BI-S3 (prox.)	GR: -70 API, DL/NL slight negative separation	A)  B) 	a) basin plain deposits (distally) b) lobe, interlobe deposits (proximally)	A) 0.05 - 0.45 m sheet-like B) ?

Figure 3.11: Sedimentological description and geometries of S10 fan environments, Main Scapa Field.

(Timbrell 1993). Meandering may also be forced by lobe topography, occasionally resulting in abrupt changes in direction (e.g. Navy Fan: Normark *et al.* 1979; Timbrell 1993). The CH 2 deposits (9% of S10) form mostly isolated features interbedded with lobe and rare OB deposits (fig. 3.12). Channel stacking is rare (e.g. E5Y: CH2/CH2; E1: CH2/CH1/CH2).

Boote & Gustav (1987) identified a variety of different channel types making up the bulk of the SSM. For the S10 interval two types were differentiated but if channel CH1 and CH2 sequences really represent different channels types, i.e. braided and meandering, is speculative. For one, well control is not tight enough to establish the true nature of the channels, but also the flow conditions leading to meandering or branching submarine turbidite channels are poorly known at present (Mutti & Normark 1987; Shanmugam 2000). A rapid vertical alternation in depositional style between the two “end-members” meandering and braided, however, is probably unlikely (e.g. E1 CH2/CH1/CH2). The observed sudden plugging of channels or channel segments by debris flow and other deposits, i.e. CH 1 infill, forcing channel avulsion may occur in both meandering or braided channel types (Clark & Pickering 1996). Rescoursing and/or reestablishment of channels in other locations by renewed turbidity current activity after channel plugging is likely (e.g. Frigg Field: Helland *et al.* 2002).

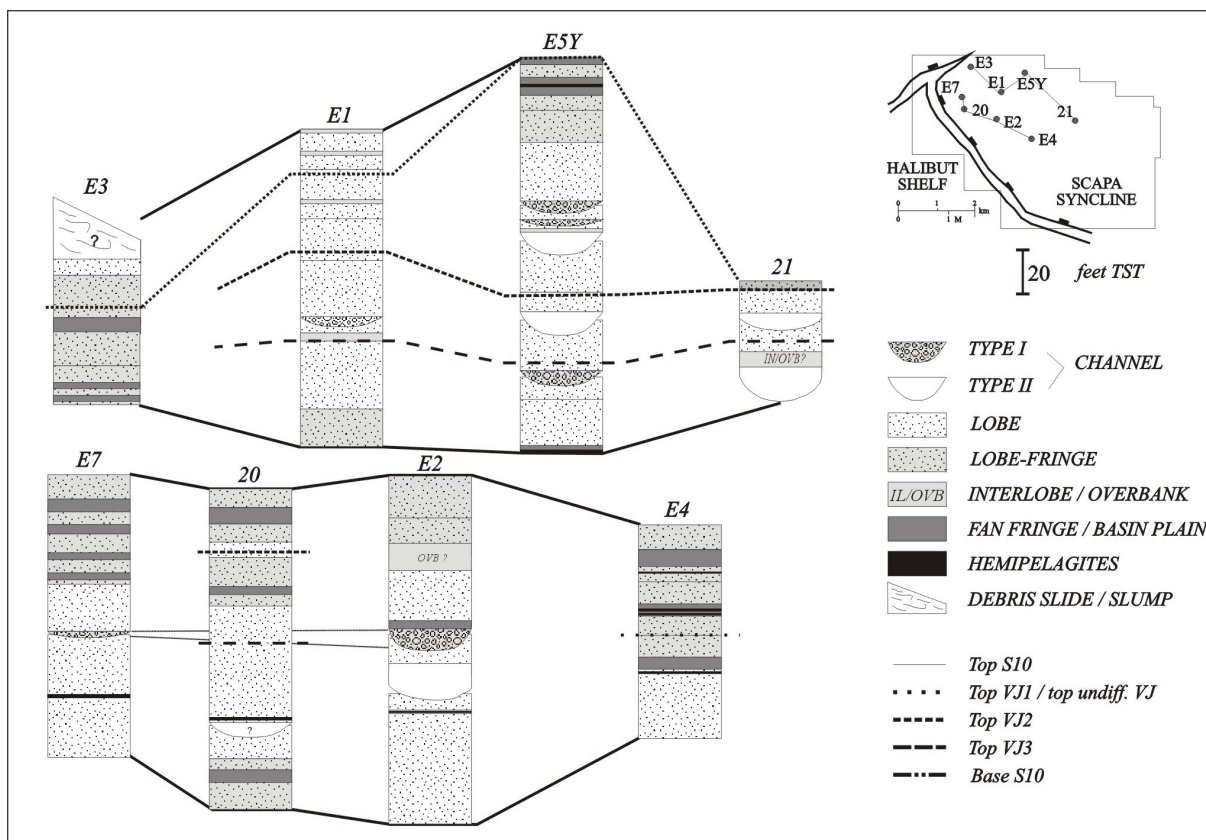


Figure 3.12: Spatial and temporal distribution of fan environments within the S10 interval, Main Scapa Field..

The distributary channels are associated with non-channelized sandy deposits and occasionally channel-related (overbank) deposits which would suggest a channel-lobe transition or proximal lobe environment (*sensu* Mutti & Normark 1987; 1991). However, channel-fill deposits are identified in proximal as well as distal positions (e.g. 21, E5Y; fig. 3.12) and at one stage near shelf-parallel fairways developed (E2-E7). Their distribution in time and space (fig. 3.12) paired with an apparent lack of a clear proximal-distal trend, suggests a complex network of pathways feeding the S10 system driven by upstream switching of feeder activity and fault-controlled sea-floor topography capturing flows thus allowing preferential pathways to bypass proximal depositional locations funneling sediment further into the basin (McAfee 1993; see *chapter 3.4*). Discrete channeling with occasional overbank formation may form but channeling also may well be less distinct developing along existing topographic lows.

The thick debrites encountered in well E3, containing shell fragments and reworked carbonate nodules and turbiditic sandstones probably represents reworked, semi-lithified Scapa deposits originating from along the West Scapa Fault (Hendry 1994). They probably represent localised bulges of debrite posing obstacles on which shelf-scoured S10 turbidites probably deflected and/or onlaped and/or ponded (Kneller 1995).

3.3.2 Non-channelized sand-dominated deposits

The bulk of the S10 interval is made up of sandy, non-channelized deposits (74 %). They are dominantly composed of S and minor GS and SM facies. Based on differing sand/shale ratio, bed thickness pattern, dominant grain size and dominant lithofacies type and association, the deposits can be classed as lobe and lobe fringe deposits (*sensu* Mutti & Normark 1987, 1991; fig. 3.11).

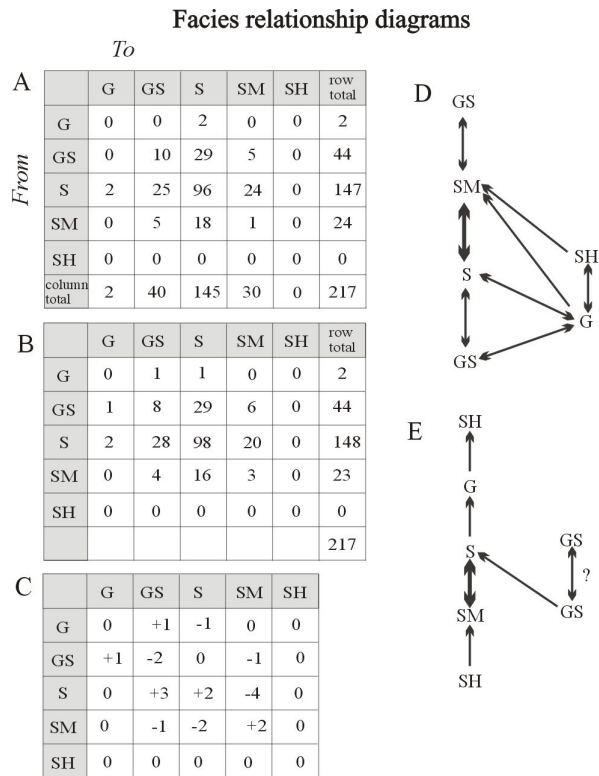


Figure 3.13: Facies relationship diagram for S10 lobe deposits: A) observed data array of bed transitions. Lithology recorded at the top of columns overlies those recorded in the rows. B) predicted data array assuming a random arrangement of lithologies. Calculated by cross-multiplying the rows and column totals of the data array and dividing by 217 (the total sample). C) differences between the observed number of transitions a) and the predicted number, assuming a random arrangement b). D) facies relationship diagram showing the most common upward and downward transitions for each lithology. E) facies relationship diagram showing the largest number of up- and downward transitions that occur for each lithology after subtracting those predicted if the beds were randomly arranged.

a) Lobe deposits

The lobe deposits (47 % of S10) are characterised by average sand/shale ratios of 9.5:1. Individual lobe packages are 2.5 - 21 m thick, composed of 0.40 - 0.80 m thick beds (fig. 3.11; enclosure 1), occasionally containing up to 4 m thick, commonly amalgamated megabeds akin to DWMS (deep water massive sands) of Stow & Johansson (2000) (e.g. E5Y: 9313-9326 ft). Erosion is rare (8 %, e.g. E1: 9171 ft) which is believed to result from solemarks and/or small localised scouring. The lobes are composed of dominantly S1-3 (> 60%) and varying amounts of GS1-4 facies, interbedded with rare thin-bedded SM2/SM3 turbidites. Occasionally, they are dominated by up to 75 % GS facies (e.g. E5Y: 9456 – 9423 ft [TL 2/3]; E7: 9931 - 9894 ft [TL 1/2]). The most common facies associations* are S – S (44 %), GS – S (13.4 %), S – GS (11.5 %), S – SM (11 %) (fig. 3.13). The mostly normally graded beds (78 %) usually contain little overall clay content (~ 5 vol.%), which is typically concentrated at the top of beds ($T_{d,e}$ of Bouma 1962). Here, bioturbation is particularly common (38 %, Zoophycus, Teichichnus, Planolites: enclosure 1). Syndimentary dewatering structures (11 %). And some soft-sediment deformation indicating loading or slumping are occasionally present.

Internally, the lobes are composed of 0.6 – 2.4 m thick, 2 - 4 bed thinning-/fining or thickening-/coarsening upward sequences, (fig. 3.11; 3.14) arranged to form crude 4 – 11 m thick asymmetric coarsening- and thickening-upward (42 %; e.g. E1: S – S/GS at 9255 – 9218 ft [TL 2]; E5Y: fs – ms S

* Facies associations are groups of facies that occur together and are considered to be genetically or environmentally related (Reading 1996). Common pitfalls in facies transition diagram analysis include stressing more common sequences, while the statistically insignificant, but geologically important ones are subordinated, i.e. misinterpretation of erosional or non-erosional contacts which provide important clues for the environmental interpretation (Reading 1986) and oversimplification by using lithofacies groups (n=6) rather than types (n=20) disregarding the true complexity of the system.

at 9336 – 9305 [TL 8/9]) or thinning- fining-upward sequences (28 %; e.g. well 21: 10537 - 10523 ft [TL 4]). The remainder are randomly arranged. The high amount of 2-bed sequences is believed to result from variations in flow volume, competence, thickness and/or topographic compensation (e.g. Mutti & Sonnino 1981; Kneller 1995; Chen & Hiscott 1999a) while the larger thickening- and coarsening upward sequences are believed to be generated by lobe progradation (e.g. Mutti & Ricci Lucchi 1972; Ricci Lucchi 1975b; Shanmugam & Muiola 1991; Mutti & Normark 1987, 1991). The observed random or thinning-fining upward patterns, however, may result from lobe aggradation (e.g. Ricci Lucchi & Valmori 1980; Hiscott 1981), retrogradation (*chapter 2.4.*) or interacting flows from different sources which may superimpose and overprint each other leaving no clear pattern (Heller & Dickinson 1985).

In wireline logs, the sandy lobe deposits are generally characterised by low GR values, often showing an upward decrease or increase in API values reflecting changing sand/shale ratio which are commonly interpreted to record coarsening-upward sequences or fining upward sequences respectively (Rider 1996), or they show no particular trend (e.g. top E1). Density readings are very much dependent on the state of cementation and pyrite formation. Clean, oil-logged sands show low readings ($2.2 - 2.3 \text{ g/cm}^3$), while pyrite formation, for example, increases to 2.75 g/cm^3 (e.g. well E2: 9131 ft).

Like the lobe deposits described in the E-Fan of the Cingöz Formation (*chapter 2.4*), the Scapa lobes do not fit the classical depositional lobe model *sensu* Mutti & Normark (1987) where lobes form isolated bodies within mudstones or finer-grained, thinner-bedded turbidite deposits. The analysis of the Scapa lobes and the distribution of the fan components (fig. 3.12) indicates that classical proximal-distal trends as encountered in other fan systems, involving grain size and bed thickness decrease while internal organisation and shale content increase (e.g. Macigno Formation: Ghibaudo 1980; Kongsfjord Formation: Pickering 1981; Eocene Hecho Group: Mutti & Normark 1987; Rocchetta Formation: Cazzola *et al.* 1981; *chapter 2.4*) are absent in the S10 interval. On the contrary, a complex interdigitation of lithofacies and fan components exists resulting in a rather distinct central *versus* lateral depositional and varied vertical trends. The crudely defined S10 lobes form mostly isolated, occasionally stacked features (e.g. top E1) associated with channel, OB, lobe fringe or occasionally fan fringe deposits (fig. 3.12). While the shallow channels erosively cut into lobe deposits, other contacts are either gradational (lobe fringe) or sharp (OB; enclosure 1). Their association with shallow distributary channel-fill/OB deposits indicates a relatively proximal lobe depositional environment (e.g. *chapter 2.4.2*), the S10 component distribution, however, defies this simplified interpretation. Mutti & Normark (1987, 1991) believe these type of lobes to generally be of sheet-like geometry but of smaller areal extent. These “proximal” lobes are especially prominent in the central wells (E2, E1, E5Y) and to a lesser extent in the western proximal wells (20, E7; fig. 3.15). Well 21 to the distal east is an exception (fig. 3.12). Otherwise, lobes become increasingly associated with finer-grained lobe fringe / fan fringe deposits (E3, E4, top E5Y) suggesting more distal/marginal positions within the system (Pickering 1981; *chapter 2.4.3*). Analysis of grain size and bed thickness trends, indicates generally

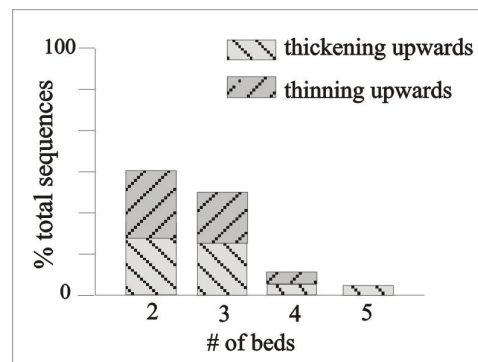


Figure 3.14: Asymmetric bed thickness pattern of S10 lobe deposits determined with 2-bed average smoothing method.

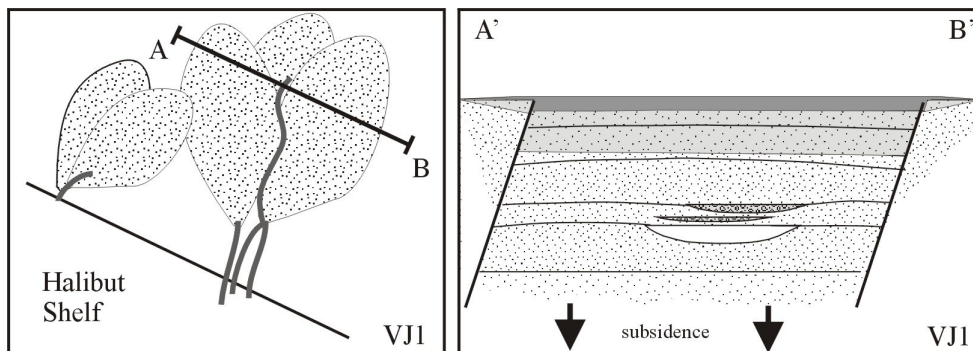


Figure 3.15: Schematic diagram showing depositional thickening in fault- and/or differential subsidence-induced intrabasinal depressions during VJ1.

coarser-grained and thicker-bedded in the E1, E5Y and E7 lobes. The contrast is especially striking in the closely spaced wells E7 (ms-vcs / mostly GS facies) and 20 (ms-cs / S facies), pointing

to potentially different source areas. Lobes in E5Y are generally coarser, but less coarse than in well E1 and may represent downcurrent equivalents of these. Correlation between wells is difficult, however, based on the fan environmental representation in space and time (fig. 3.12), none of the lobes appear to be basin-wide features but are rather of areally confined, probably elongate geometry (fig. 3.15; see *chapter 3.4.1*).

Vertically, all wells with exception of E1 and E3 display shaling-upward (fining-upward) from sandy lobe deposits to lobe fringe, interlobe and/or fan fringe/basin plain (fig. 3.12; enclosure). The basal E1, E3 and 20 are dominated by varying amounts of lobe fringe, interlobe and/or fan fringe/basin plain. Process sequence analysis (after Cronin 1994) which records flow at the time of deposition by using grain size and sedimentary structures as indicators of transport and depositional processes, confirm this trend for the cored S10 interval, almost always indicating the transition to less energetic, more tranquil depositional environments (appendix 3). This may be related to reduction in grain size in the feeder system or an increase in distance from the input point perhaps due to rising sea level (see *chapter 3.4*). Bed thickness trends as identified by RAM technique (Murray *et al.* 1996; *chapter 1.4*) partially reflect this trend. The lower part of E5Y (VJ3/VJ2) are dominated by thick units of thicker-bedded intervals, the top (VJ1) by thick units of thinner-bedded intervals, while well E1 shows a contrary trend. Wells E2 and E7, however, show less distinct organisation (appendix 4). Bed thickness is a function of flow volume rather than transport and depositional processes.

The internal organisation of the lobes is fairly crude (see *above*), it does not appear to improve towards more distal/marginal areas, although this is generally expected (e.g. Cingöz Formation: *chapter 2*; Eocene Hecho Group: Mutti & Normark 1987; Rocchetta Formation: Cazzola *et al.* 1981).

Lobe progradation, switching and overall aggradation may result in vertical stacking, representing stable depositional environments (Pickering 1981), probably in a confined space. Isolated lobes within areas of normally fan fringe sedimentation suggests episodic lobe migration into this particular area indicative of unstable depositional processes, possibly reflecting source control (Pickering 1981) or lobe switching (*chapter 2.4.3*). Seismic data indicates lobe thinning towards the shelfal area, thickening in a basinal direction, which McAfee (1993) as detached lobes *sensu* Mutti & Ricci Lucchi (1975). The development and geometries of the S10 lobe deposits appear to be governed by a combination of autocyclic control and allocyclic controls (see *chapter 3.4 for further discussion*).

b) Lobe fringe deposits

The lobe fringe deposits (28 %) form 1 - 6 m thick units of lower average sand:shale ratio (4:1; fig. 3.11). Their occurrence in core is rare, where they are characterised by fine-grained sandstones (S2/S3) and shale-rich SM (e.g. E1: S2-S3-SM2-SM3 at 9172-9177 ft; table 3.4) which are abundantly bioturbated (60 %). The thin-bedded (0.05 - 0.3 m) deposits, corresponding to intervals of below median thickness (appendix 4), are arranged in crude 2 - 6 ft fining-upward sequences composed of 2 - 4 beds.

Most of the lobe fringe deposits were identified from wireline record, where they are characterised by mostly higher API/GR readings than lobe deposits. They often form part of distinct shaling-upward or downward sequence in association with lobe and/or fan fringe deposits (shale-down/coarsening-up: lobe fringe to lobe: E1: 9278-9216 [TL 1/2]; interlobe-lobe fringe-lobe: 20: 9930-9905 [TL 3]; shaling-up/fining-up: lobe-lobe fringe-fan fringe: 20: 9790-9767 [TL 9]; E 7: 9853-9820 [TL 4-6]; enclosure 1). The contacts with lobe and fan fringe deposits are gradational in both proximal and distal locations (e.g. 20, E5Y). The lobe fringe deposits form isolated features in proximal (e.g. 20, E2, E4) and in distal / lateral position (e.g. zone VJ1: E3, E5Y) where they become increasingly more abundant (fig. 3.12).

Lobe fringes *sensu* Mutti (1977) represent the distal equivalents of coarse-grained and thick-bedded sandstone lobe deposits in both down-current and cross-current directions, representing a lateral / distal depositional environment (e.g. *chapter 2.4.3*). The deposits are of wedge-like, "fringing" geometry (fig. 3.11).

3.3.3 Shale-dominated deposits

Distinctly shale-dominated deposits (11.5 % of S10) occur in association with channel, lobe and lobe fringe deposits. They are typically composed of thin-bedded, fine-grained SM to SH facies (plate 8.5), with S facies occasionally interbedded (fig. 3.11). Preservation in core is rare (e.g. E2: SM-SM-S3-SM: 9082 ft) where they are characterised by high GR (70 API), low RT and distinct negative DL/NL separation. In the

uncored S10, shale-dominated deposits are fairly common, the higher GR values (80-135 API) suggest a higher shale content, i.e. mostly SH facies and/or very shale-rich SM facies, than observed in core.

The overall thickness ranges from 0.5 - 3 m in proximal (e.g. 20, E2, E4) to up to 5 m in distal locations (E3, E5Y). Their bases and tops are bound by sand-dominated units (fig. 3.12). They typically form the base of larger-scale 'shaling-down' (GR-) trend lines (ie. general coarsening-upward; e.g. E3: SH-SM - srS at 10745 - 10718 ft [TL 1], E4: SH-SM-srS at 9602 - 9587 ft [TL 6]; E5Y: SH/SM - srS at 9285-9272 ft [TL 11]) or the top of 'shaling-upward' (GR-) trend lines (ie. general fining-upward; e.g. 20: SM-SH at 9780 - 9763 ft [TL 9/10]; E2: srS-SM at 9077 - 9064 ft [TL 11]; E3: srS- SM-SH at 10718- 10690 ft [TL: 2]). Sharp bases and/or tops are rare (e.g. E5Y: S-SH at 9285 ft).

The association with channel, lobe and lobe fringe facies in relatively proximal fan locations (fig. 3.12) suggests their possible origin as overbank and/or interlobe deposits *sensu* Mutti (1977), with distal lobe fringe and hemipelagites a fan fringe and/or basin plain origin *sensu* Mutti (1977) and Mutti & Normark (1987) (fig. 3.11).

a) Overbank / Interlobe deposits

The fine-grained, thin-bedded, current-laminated sands and silts and graded mudstones of overbank (OB) deposits *sensu* Mutti (1977) and Mutti & Normark (1987, 1991) are found in association with channels where they form by lateral spreading of a mainly confined turbidity current (Mutti & Normark 1987, 1991). In the S10 interval, channel-lobe?-OB associations are present (e.g. well 21 at 10563 ft; E2 at 9130 ft). They form thin, irregularly bedded, maximal 0.5 - 2.1 m thick shale-dominated intercalations (fig. 3.11). The thick, distinctly bimodal SM1 facies (E2: 9070-9077 ft; 60% shale matrix, granule - pebble-sized grains, traction structures; plate 8.4) topped by SH is unique in its lithology, the high matrix content probably resulting from reworking and incorporation of shale-rich sediments into the flow. OB deposits generally possess a wedge-like geometry, thinning away from the channel (fig. 3.11; Mutti & Normark 1987; Clark & Pickering 1996).

The 0.6 - 3 m thick interlobe deposits separate thick-bedded, coarse-grained sandstone lobe and lobe fringe deposits (fig. 3.12). The contacts are transitional as part of shaling upward sequences (fining-upward?; e.g. well 20 at 9810 ft) indicating gradual lobe migration into or out of a particular area or abrupt, suggesting a sudden shift in depositional focus (e.g. E1 at 9125 ft; fig. 3.12). Interlobe deposits possess a lenticular geometry resulting from infilling of topography between lobe bulges (fig. 3.11; *chapter 2.4.3*).

The OB and interlobe deposits form approximately 3.5 % of the total S10 interval.

b) Fan fringe / basin plain deposits

In distal fan locations, up to 5 m thick, shale-dominated deposits are interbedded with distal lobe fringe sediments (fig. 3.12; e.g. E3, E4, E5Y). They are mostly identified by wireline response (fig. 3.11), where they appear to form part of shaling-upward and/or downward trends, from fan fringe to lobe fringe and *vice versa*, suggesting gradual migration of sand deposition to and/or out of these particular areas (e.g. E3: TL 1/2). Occasionally, sharp facies changes indicate a rapid shift in sand depositional locus (e.g. E5Y: 9285 ft). Fan fringe deposits are typically thin to very thin-bedded, very fine sandstone turbidites forming regularly bedded packets of sheet-like geometry (fig. 3.11; Mutti 1977; Pickering 1981), however, the fan fringe deposits of the S10 interval are very shale-rich. Occasionally, marls are interbedded with the fan fringe packages suggesting a basin plain origin (Mutti 1977; e.g. E5Y (TL1)).

The fan fringe / basin plain deposits form approximately 9 % of the S10 interval.

3.3.4 Hemipelagic marls

Hemipelagic marls (1.5 % of S10) form highly bioturbated beds of 5 - 45 cm TST with sharp bases and tops (fig. 3.11). Occasionally, they comprise mm-thick silt and very fine sand laminae. Marls are rare in the cored and uncored sections of the S10 interval (e.g. cored: wells 21, E2, E5Y; uncored: E4). They are commonly interbedded with SM / SH facies (e.g. E2: SM3-BI-SH at 9163 ft [plate 8.6]; E5Y: BI-SM3 at 9495 ft) or occasionally S facies (E7: S2-BI-S3 at 9893 ft).

The marl beds bear a striking resemblance to the marly clasts contained in the debrites and gravely high-density turbidite deposits (well 21 at 10585 ft), believed to derive from erosional unroofing at the fault scarp and/or shelfal environment (Hendry 1994; McAfee 1993). The marl beds in association SM/SH facies (e.g.

E2, E5Y) formed *in situ* while clastic sedimentation was temporarily suspended, pointing to an overall high carbonate background sedimentation (Harker & Chermak 1992). In distal locations, the marls are associated with basin plain / fan fringe deposits (e.g. E5Y, E4; fig. 3.12) while in relative proximal positions, the marls are associated with overbank / interlobe deposits and occasional lobe fringe deposits (e.g. E2, E7). In the latter locations, rapid shift in the depositional focus in the respective fan area probably resulted in a spatially confined temporary suspension in clastic sedimentation, resulting in a lensing depositional geometry. The distal marls mark the distal depositional limit of the S10 system at that particular point in time. They form laterally more extensive, sheet-like deposits (fig. 3.11).

3.4 Lobe Accumulation

The size and appearance of lobe deposits is a function of the size of the system, the basin size and its configuration and the volume of individual turbidity currents, grain size and many other factors. Lobe deposits can therefore have very different dimensions and shapes (Mutti & Normark 1987, 1991) which may change through time with changing controlling parameters. Scapa lobe accumulation needs to be viewed within the context of the overall development of the S10 system, which can be described in 4 separate stages: zones VJ (subzones VJ3-1) and VI (fig. 3.16).

3.4.1 Temporal and spatial development of the S10 Interval

VJ3 subzone

Deposition took place throughout the Main Scapa Field. The greatest depositional thickness was reached in central-western well 20 (92 ft TST), gradually declining towards the central-north (E5Y) and east (21) (fig. 3.16a). The depositional limit is delineated to the south by the conglomeratic wedge fringing the Halibut Shelf and the Claymore High to the north (Riley *et al.* 1992). To the west deposition takes place in the West Scapa Field occur, while the eastern depositional extend is unknown.

Channelized deposition in the east (21) started during the S9 interval (McAfee 1993) continues into VJ3. This eastern part of the field is probably fed by a source located further to the south (feeder area 1*). The central field area is underlain by shale-rich lobe fringe and/or fan fringe/basin plain deposits (S9 interval) which are now sharply overlain by sand and gravel-dominated lobe and channel-fill deposits (e.g. E1, proposed VJ3 zone of E2; E4; E5Y). Shifting depositional focus by lateral, westward? lobe migration (20, E1?) and/or fan progradation towards the basin (E5Y, E1?) in conjunction with (re-)activation of a southern source area feeding sediment into the central field (feeder area 2) are probably responsible for the high depositional thickness in the central axis (20-E2-E1-E5Y). Laterally, lobe deposits thin and fine (SE: E4) to lobe fringe and fan fringe/basin plain sedimentation (NW: E3). The proximal western area (E7) is dominated by coarse lobe deposition, probably sourced by a westerly lying source (feeder area 3?).

VJ2 subzone

Depositional trends established during VJ3 continues during subzone VJ2 (fig. 3.16b), however, sediment accumulation is much more uniform, ranging between 48.4 ft TST in the west (20) to 25 ft TST in the east (21). Lobe and channel-fill deposition dominate the central axis (20-E2?-E1-E5Y) and the east (21). Locally shifting depositional locus results in lobe migration (e.g. well 20: lobe/lobe fringe/interlobe). The SE (E4) is gradually dominated by shale-rich lobe fringe sedimentation which may be associated with either feeder area 1 or 2. In the NW (E3) fan fringe/basin plain deposition continues to dominate.

Deposition in the W (E7) is probably still dominated by lobe deposition. Shelf-parallel development of a distributary system suggests westward shifting sediment locus. Laterally coalescing deposition from different scoures (feeder area 2/3) is likely in the western syncline.

* the term “feeder area” instead of “feeder” is used to indicate that possibly a multitude of smaller feeders located in close proximity rather than a single, larger feeder conveyed material into the syncline.

VJ1 subzone

Marked areally restricted deposition in connection with extreme thickness variations characterise subzone VJ1 (fig. 3.15c). 178 ft TST of sediments accumulated in the central-north of the field (E5Y) rapidly declining towards the centre (E1: 49 ft) and east (21: 4.5 ft). VJ1 deposits are absent in proximal areas (20) and undifferentiated in the remaining wells.

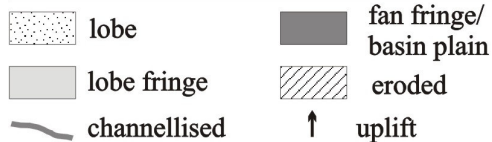
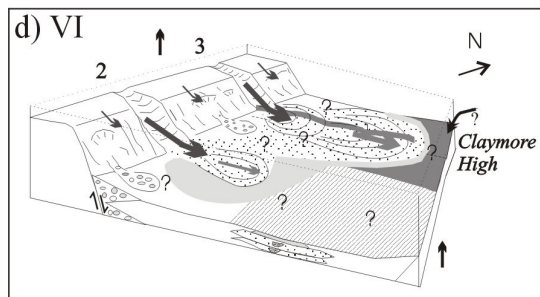
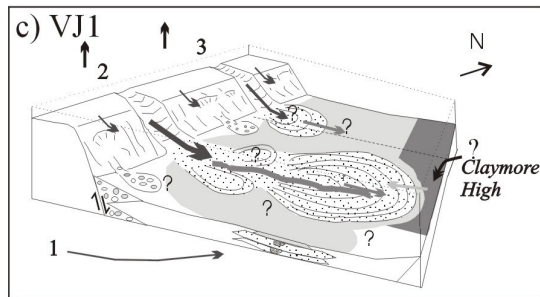
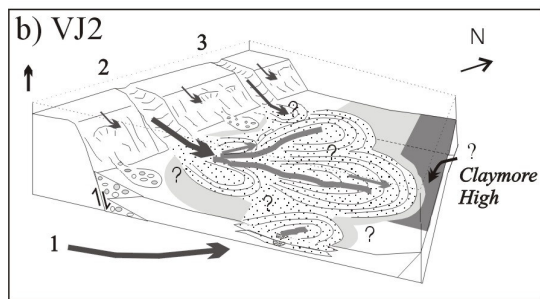
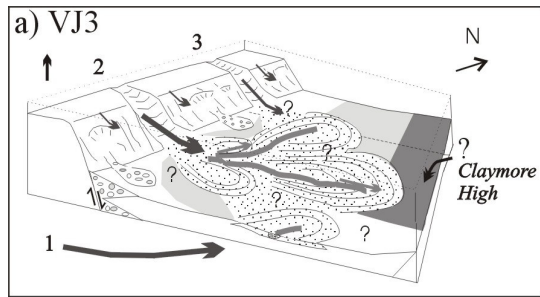


Figure 3.16: The spatial and temporal reconstruction of the S10 interval reveals changing feeder activity exerting a major influence on the locus of deposition.

In the east (21) thin lobe fringe deposition marks the decreased sediment influx from feeder area 1 resulting in retreating or migrating? lobe deposition. Shale-rich lobe fringe deposition probably continued in the NW and SE (undifferentiated zone VJ wells E3/E4). The central-north (E5Y) is dominated by coarse-grained lobe and channel-fill deposition, progressively fining and thinning to lobe fringe and fan fringe / basin plain deposition, while lobe deposition continues to be prominent in the centre (E1; fig. 16c). The extreme sediment accumulation in well E5Y may result from a combination of a fault-controlled? differential subsidence creating a local intrabasinal low compounded by sediment ponding and contribution from the Claymore High (see chapter 3.4.2: controls).

The absence of VJ1 deposits in proximal well 20 cannot merely be explained by temporary suspension of clastic deposition in this area resulting from a shift in the depositional locus. Due to the high carbonate background sedimentation (Harker & Chermak 1992) at least marls should have formed. It is thus likely that SM/SH or marl deposits were subsequently eroded.

VI zone

Deposition appears even more areally restricted, essentially resulting in two sandstone depositional areas (fig. 3.16d):

- i) in the central field area, lobe deposition dominates the southeast (E4: 67 ft), thinning and shaling to lobe (E1: 32.5 ft) and lobe fringe (20: 37 ft) sedimentation in central-proximal direction. The sediments are very likely sourced from feeder area 2. The SE shift in depositional locus probably is driven by antecedent depositional topography.
- ii) lobe deposition progrades north, suggesting feeder area 3 becoming increasingly active while intraformational breccias (E3) point to periods of intrabasinal tectonic instability in the north-western syncline.

Sedimentation from feeder area 1 appears to have ceased. No VI deposits are recorded in the E (21). Equally, VJ deposits are absent in the central-north (E5Y) is conspicuous. It is believed that initial hemipelagic and/or basin plain deposition took place, but differential uplift

in the NE and E led to their erosion (see chapter 3.4.2).

McAfee (1993) suggest renewed conglomeratic progradation into the basin whereas this study interpreted a lobe depositional environment for the uncored VI of well E4.

3.4.2 Controls

3.4.2.1 Basin physiography, geometry and seafloor topography

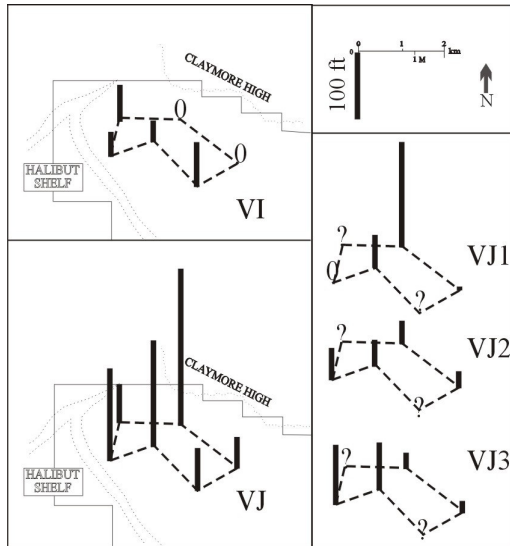


Figure 3.17: Thickness distribution of S10 zones and subzones projected into Main Scapa Field. Basin topography not considered.

al. 1991 believe differential compaction taking effect in the Hauterivian to be responsible for the synclinal geometry of the Scapa basin, where the conglomerates showed lesser compaction than the finer-grained basinal deposits. Within the basin, the underlying S9 shales were likely to form depressions probably enhanced through their syndimentary differential compaction (average compaction rates: shales 60 %, sands 20 % from Stow & Johansson 2000; e.g. Frigg Field: Heritier *et al.* 1978) while the sandy channelized / non-channelized S9 deposits formed topographic features. This “subcrop” lithology thus influences the accommodation space available for sand accumulation (e.g. Fladen Ground Spur: Freer *et al.* 1996; Rona Member/West Shetland Basin: Verstralen *et al.* 1995).

Throughout the S10, major variations in sedimentary thickness are conspicuous (fig. 3.17). Especially subzone VJ1 records extreme sediment accumulation in the central area (E2-E1-E5Y), dramatically thinning to the southeast and northwest respectively (fig. 3.17). A major NE-SW-running normal fault, the Mid Scapa Fault, is recognised to the west of the E2-E1-E5Y-line (fig. 3.18) and the existence of minor, parallel faults suggested throughout the syncline (McAfee 1993). McGann *et al.* (1991) observed fault movement along these reactivated Caledonian fault trends, however, less significant than concurrent faulting (i.e. Halibut Shelf fault), and very little throughout the Scapa Sandstone Member. However, even subtle fault-

Basin configuration, faulted and depositional topography exert a critical influence on original and preserved sandstone thickness and geometry of lobe deposits (e.g. Normark *et al.* 1993; Reading & Richards 1994; Schuppers 1995). The Scapa sediments were funnelled via multiple feeders from the southern Halibut Shelf into a small, maximal 4 x 8 km wide, fault-bounded basin (Oakman & Partington 1998). To the north and east the syncline was bound by the steep ramp of the Claymore High and the West Scapa Fault respectively while it extends further to the southeast as the Scapa-Highlander subbasin (McGann *et al.* 1991). A transfer zone to the Northern Claymore Area in the northwest allowed sediment transfer further into the basin during the Hauterivian (Harker & Chermak 1992).

The pre-S10 basin was marked by a heterogeneous system with thick sand and gravel deposits in the east (21), becoming sandier towards the central direction (E4). The north and west are underlain by thick units of shaly and marly hemipelagic deposits (E5Y, E3, 20). The debrites of the 200 – 700 m wide conglomeratic wedge shaped the physiography of slope/base-of-slope (fig. 3.7). McGann *et*

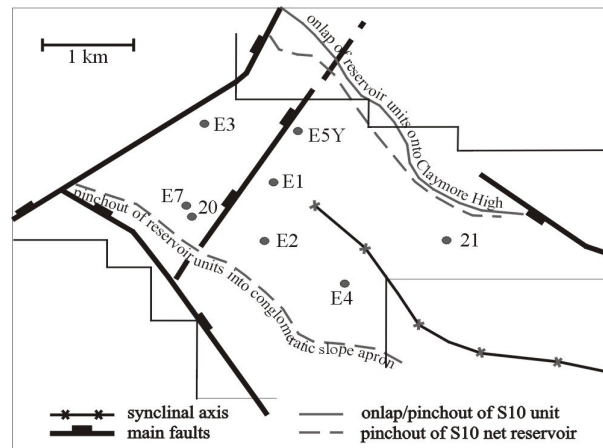


Figure 3.18: Main structural elements of the Main Scapa Field.

scarp topography and/or synsedimentary differential subsidence of fault-controlled basin sectors creating intrabasinal depressions may have forced preferred funnelling of sediments thus allowing for locally enhanced sediment accumulation, e.g. zone VJ1 of E5Y. The stacked, aggradational style of the primarily non-channelized, sheet-like sandy deposits together with the narrow, elongated depositional geometry further points to deposition in a confined setting. Similar controls on sediment accumulation are recorded in other deep-water clastic systems, for example, the Cingöz Formation/Turkey (*chapter 2*), Arktinos Sandstone/Greece (Schuppers 1995), Northern Area Claymore (Kane *et al.* 2002) and the Brae Field (Stow 1995b; *further examples: chapter 2.5.1*).

McAfee (1993) and Hendry (1994) believe sediment to have ponded against the Claymore High which acted as a barrier resulting in flow decrease leading to deposition of predominantly massive sand bodies (e.g. DWMS at top of cored E5Y; Kneller 1995; Gryphon Field: Purvis *et al.* 2002). This together with sediment input from the Claymore High (Hendry 1994) and axial deflection (McAfee 1993) may have further contributed to more localised deposition, especially close to the high.

Topography resulting from antecedent sediment deposition affected Scapa lobe accumulation at various scales:

- i) microsequences (up to 2.4 m; *chapter 3.3.2*) resulting from topographic irregularities are especially common in proximal lobe deposits (e.g. Normark *et al.* 1979; Mutti & Normark 1991; *chapter 2.4.2.1*).
- ii) macrosequences (2.5 - 21 m) at mostly asymmetric “intra” (i.e. individual lobes; E5Y, E7 enclosure 1) and “inter” lobe-scale (i.e. stacked lobes; E1, E2, E5Y) resulting from lobe migration, i.e. autocyclic lobe switching due to preceding topography and/or channel avulsion or allocyclic controls (e.g. Heritier *et al.* 1978; Pickering 1981; Normark *et al.* 1993; Bouma 2000; Garland *et al.* 1999) creating an offset-stacking pattern at lobe-scale.

Mass wasting events in shelfal areas or swamping of conduits can lead to the reconfiguration of the basin floor topography and shelfal physiography (Cronin *et al.* 1998). Intraformational debris flow deposits found in the north of the field (E3) and reported from other areas proximal to the faulted shelf margin (e.g. McAfee 1993; Hendry 1994) are very likely to have formed localised depositional buldges presenting further obstacles to flow forcing deflection (e.g. Kneller 1995) and/or plugging sediment pathways (e.g. CH I-fill; e.g. Reynolds & Gorskine 1987).

3.4.2.2 Tectonism

The Scapa-Highlander half-graben created under Late Jurassic transtensional conditions was exaggerated during the Late Cimmerian transpressional regime by inversion of older Jurassic structures above sea level (Oakman & Partington 1998) initiating clastic sedimentation in the Scapa syncline (Harker *et al.* 1987). Tectonism shaped the narrow, elongate basin geometry, basinfloor topography as well as dictating sediment pathways across the Halibut Shelf probably along tectonic lineaments (Boote & Gustav 1987; McGann *et al.* 1991; McAfee 1993; *chapter 3.4.2.1*) thus actively controlling the location of sediment accumulation within the basin (McAfee 1993). Deposition of the Scapa Sandstone Member (SSM) was affected by different stages of Late Cimmerian tectonism (K20/K30 of Jeremiah 2000; fig. 3.19) resulting in phases of high sediment input (units SA and SD) and shifting depocentres (Harker & Chermak 1992). Partial erosion of unit SA in the southeast of the field points to differential uplift within the syncline during the late Valanginian – early Hauterivian boundary (fig. 3.19), the so-called “Lower Valanginian Unconformity” (O’Driscoll *et al.* 1990) or “Late Valanginian event” (Riley *et al.* 1992).

Source-area tectonism lead to renewed and/or increased clastic deposition in the central Main Scapa Field (wells 20, E2, E2, E5Y). The observed northwestward migration of the depositional locus appears to be directly controlled by differential source area uplift driving the shift in feeder activity from the south east (feeder area 1) to northwest (feeder area 3) (fig. 3.16; *chapter 3.4.1*). Source area control expressed in shifting feeder activity is frequently encountered in deep-water clastic systems of active basins (e.g. Cingöz Formation: *chapter 2.5*; Paola Basin systems: Trincardi *et al.* 1995) which Stow (1985b: South Brae Field) illustratively termed “piano-key tectonics”. Hendry (1994) believes that source area uplift is additionally responsible for facies distribution within the SSM by controlling the nature of material reworked into the basin. This may lead to, for example, varying grain sizes in similar fan locations, such as the coarse sands of

well E7 and fine to medium-grained sands of well 20. Reoccurring seismic activity was most likely responsible for triggering frequent mass wasting events directly off the fault-scarp in the south (e.g. well E5; McAfee 1993), forming the conglomeratic slope apron and occasionally leading to intraformational debrites and slides in the northwest (well E3) and throughout the field (McAfee 1993; Hendry 1994).

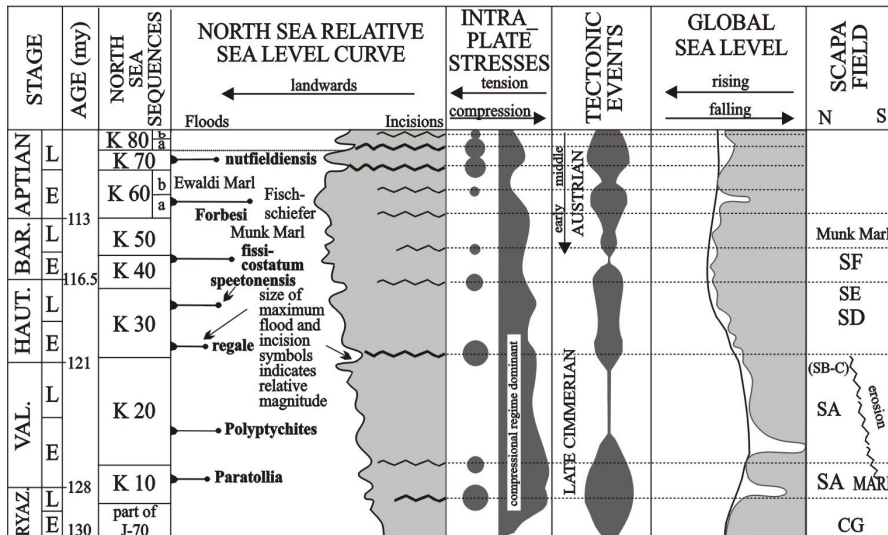


Figure 3.19: North Sea relative sea-level curve. Calibration of maximum flooding surfaces and eustatic sea-level oscillations with Late Cimmerian and Austrian tectonism that affected the North Sea Basin (modified from Jeremiah 2000). CG, SA-SF nomenclature after McGann *et al.* (1991). EE = erosional event corresponding to Lower Valangian unconformity of O’Driscoll *et al.* (1991) and Late Valangian event of Riley *et al.* (1992).

Tectonism also appears to have affected the S10 accommodation space. On the one hand, differential subsidence of closely spaced basin sectors resulted in localised enhanced thickness accumulation (*see* 3.4.2.3), on the other hand, in an environment with high carbonate background sedimentation (Harker *et al.* 1993) hemipelagic marl deposition should be expected if clastic sedimentation was temporarily suspended and thus the absence of zone VJ1 deposits in proximal well 20, zone VI deposits in wells E5Y and 21 indicate (renewed?) uplift and subsequent erosion in proximal (well 20) and particularly the northern-southern basin sector (wells E5Y, 21). If this distal uplift was in relation to movement of the Claymore High “pop-up” structure is speculative.

Although evidence suggests occasional uplift and local erosion within the Scapa syncline, basin subsidence is generally assumed for the time of deposition of the Valhall Formation. By the end of the Barremian, diminished tectonic activity combined with increased regional subsidence led to base level erosion and overstepping of the Halibut Horst ending clastic sedimentation (Boote & Gustav 1987).

3.4.2.3 Rate, type and source of sedimentary supply

The broadly slope parallel arrangement of marked bimodal facies points to different sediment sources and modes of deposition. The poorly sorted, 200 – 700 m wide apron of coarse debris fringing the Halibut Shelf results largely from mechanical slope destruction of the Halibut Shelf margin commencing in Late Ryazanian times (Boote & Gustav 1987; McAfee 1993) which in a basinward direction interfinger with SSM clastics (Riley *et al.* 1992).

The main source of the sandy SSM is believed to be the 10 – 20 km wide, shallow marine, high energy, high productivity Halibut Shelf, where predeposited Permian to Early Cretaceous sediments were eroded (Hancock 1990; Riley *et al.* 1992; Hendry 1994). Limited grain size ranges for both bioclastic and siliciclastic components imply some hydrodynamic sorting in the source area, prior to incorporation of the sands into gravity flows (Hendry 1994). Devonian Old Red Sandstone and older granitic intrusions were probably exposed on the Halibut Horst (Andrews *et al.* 1990) forming a significant, probably local terrestrial source. Additionally, dispersed vascular plant fragments, woody and coal debris are found throughout the SSM. It is uncertain, however, when the shelf was established, what the exact nature of the hinterland and sediment pathways were (Hendry 1994). Mass wasting on the fault-scarp provided additional locally-sourced sediments to the syncline (Boote & Gustav 1987) as well as minor sediment input from the Claymore High in the north (Hendry 1994). Occasionally tuffs, now preserved as green shales, were “shed” into the basin.

Off-shelf transport is typically controlled by a combination of river discharge, margin circulation and shelf sediment resuspension, the latter dominantly forced by tidal or storm wave activity and in times of river floods (e.g. Puig *et al.* 2003), while seismic activity is also known to trigger mass wasting events (e.g. Lebreiro *et al.* 1997). Hendry (1994) believes a combination of tectonism and storm wave activity to be responsible for the massive influx of poorly consolidated sands into the Scapa syncline.

The sediments were shed into an approximately 500 ft deep basin (O'Driscoll *et al.* 1990) of relatively warm waters (temperature ~14°C; Hendry 1994) while an overall seasonal climate prevailed (Hancock 1990). During the 8 myr of near continuous clastic SSM deposition (Oakman & Partington 1998), 179 m of sediments accumulated, averaging sedimentation rates of 0.02 m / 1000 years. However, the S10 interval is marked by strongly varying sediment accumulation between 15.5 - 77 m (fig. 3.17).

The analysis of the S10 deposits suggests that the bulk of the sediments was derived from gravely to sandy high-density turbiditic flows and subsequently diluted flows as indicated by the high number of fining-upwards at bed-scale. Some of the encountered massive deep-water sandstones (DWMS *sensu* Stow & Johansson 2000) may be the result of sandy debris flows. Gravely debris flow deposits are mostly confined to channel-fill sequences (CH I/CH II), while fault-scarp sourced debris flows, intraformational breccias (E3) and slumping indicate seismic activity and/or failure due to rapid sediment build-up (McAfee 1993; Hendry 1994). These may pose local obstacles to flow (Kneller 1995). The greater fossil diversity encountered in the conglomerates and pebbly sandstones points to a different and lower energy part of the source region than for the sands (Hendry 1994) indicating that grain size and composition are largely source-determined. Mud-rich sequences close to the steeply dipping faulted margin (e.g. well 20, E2) indicate sediment bypass with the bulk of the sands being deposited further into the basin (McAfee 1993). The origin of the frequently observed traction structures causes debate, McGann *et al.* (1991) believe them to result from bottom current reworking while Hendry (1994) and this study (fig. 3.8) advocate their primary depositional origin. Oxic bottom waters and localised low sediment input allowed for highly bioturbated deposits. Temporary suspension of clastic sedimentation resulted in the deposition of hemipelagic marls (e.g. well E2; E4, E5Y) and in more distal parts of the basin (McGann *et al.* 1991).

The incoming sediment was of sufficient volume to onlap and/or pond against and/or be deflected by the Claymore High. Sediment bypass in the north led to the deposition of Northern Claymore Area turbidites which are, however, sourced from a different source than SSM/S10 deposits (McAfee 1993; Hendry 1994). The full extend to the northwest has yet to be determined (McGann *et al.* 1991) while the southeastern Cretaceous turbidites of the Highlander Field may be correlatives of the SSM (Hendry 1994).

3.4.2.4 Sea level changes

The Scapa Sandstone Member was deposited under a gradually rising sea level intercepted by a mildly regressive phase in the mid-latest Hauterivian (Rawson & Riley 1982). Eventually rising sea level cut off clastic sediment supply during intra-zone VG (Late Hauterivian) drowning source areas and trapping sediment on the shelf while marls and limestones of the upper Valhall Formation blanketed the entire area (O'Driscoll *et al.* 1990; Riley *et al.* 1992). A number of North Sea deep-water clastic systems also developed during rising sea level e.g. Brae turbidite system: Stow 1985b, Balder Formation/Gryphon Field: Dixon & Pearce (1995); Purvis *et al.* (2002), Rona Member/West Shetland Basin: Verstralen *et al.* (1995); Frigg Submarine Fan: Helland *et al.* (2002). Previous workers (e.g. Harker & Chermak 1992; Hendry 1994) found the "Vailian" sequence stratigraphy not applicable to the Scapa depositional system as substantial clastic deposition within the overall carbonate system of the Valhall Formation classify "lowstand systems tract", while eustatic sea-level rise for the Neocomian is well-documented. Tectonism has been recognised as the fundamental control in driving clastic sedimentation throughout the North Sea (Harker & Chermak 1992) which led Jeremiah (2000) to establish a tectonic stratigraphy for the Outer Moray Firth (fig. 3.19). Relative sea-level changes may occur over short time frames (< 100 kyr) in response to both eustasy and tectonism (e.g. Posamentier *et al.* 1988; Normark *et al.* 1993; Bouma 2001). These higher-order fluctuations may influence the distribution of sandstones, i.e. through progradation and retrogradation, and the internal architecture of components of the deep-water clastic system, e.g. fining or coarsening-upward sequences.

Local tectonism along the Halibut Shelf was probably responsible for overriding eustatic control on deposition of the SSM. Differential source area uplift resulted in localised sea-level lowering exposing large volumes of shallow marine sediment to erosion by wave activity (McAfee 1993; Hendry 1994) leading to:

- i) the overall renewed sand progradation in central Scapa Field during the S10 interval
- ii) the observed northward shifting depositional locus
- iii) fining upward at lobe and well-scale (e.g. E5Y, E7, E2, 20, E4) indicating a deepening source area, while the distinct coarsening-upward encountered in wells E3 or continuous sandy deposition in well E1 suggest the localised overriding tectonic control on sedimentation.
- iv) repetition of fine-grained facies (fan fringe-fan fringe: top E5Y: VJ and E4, E7: VI) may simply related to autocyclic mechanisms (e.g. lobe switching) or suggest small-scale sea-level fluctuations during deposition.
- v) Localised reduced sections (missing latest early Hauterivian/zone VI: E5Y, 21) indicates intrabasinal uplift and thus localised sea level changes, exposing predeposited S10 sediments to erosion.

Thus the overall rising sea level during the SSM is punctuated by localised sea-level lowering as a direct result of source area and intrabasinal tectonics controlling sediment transfer into the syncline.

3.5 Discussion

3.5.1 Interwell correlation

Prior to Riley's *et al.* (1992) introduction of a biostratigraphic correlation scheme subdividing the SSM into a number of palynological zones (VG-VR), workers had utilised lithofacies in conjunction with wireline-based correlation between wells. This resulted in the establishment of diachronous reservoir / non-reservoir units SA-SF (O'Driscoll *et al.* 1990) leading to somewhat biased environmental reconstructions overemphasising the sandy reservoir intervals in comparison to their contemporaneous shale-rich and tight sandy non-reservoir deposits (e.g. McAfee 1993).

The correlatability of individual beds principally depends upon the volume of sediment supplied and the number of entry points to a system (Lebreiro *et al.* 1997), accordingly the S10 system (zones VJ/VI), which is characterised by marked temporally and spatially restricted sediment accumulation sourced by multiple feeders, no field-wide laterally continuous marker beds can be expected. Attempted correlation at lobe / bed packet scale between adjacent wells (e.g. E2/E1/E5Y) which appear to be sourced from the same feeder area, using, for example, presence and abundance of coal fragments and bioturbation, bed thickness patterns etc. (appendix 5) did not yield satisfactory results due to rather random patterns. Only, the biostratigraphic correlation appears to be reliable as far as its resolution, i.e. zone/subzone level and base/top boundaries, permits.

The presence of tuffs (green shales) is not extensive enough to permit tuff profiling and correlation across the S10 interval, a method which in conjunction with desanded profiles proved to support petrophysical correlation in other North Sea fields, e.g. Balder Formation (Hatton *et al.* 1992).

3.5.2 Depositional model and controls

Different depositional models have been suggested to fit the SSM such as sand-rich submarine fan (Boote & Gustav 1987), sand-rich slope apron (McAfee 1993), sand-rich submarine ramp system (Hendry 1994) and proximal basin-slope to basin-floor conglomeratic and sandy aprons (Oakman & Partington 1998). Although the S10 interval represents only a "time-slice" of the SSM, it appears to reflect controls and processes dominant throughout (e.g. Harker & Chermak 1992; Riley *et al.* 1992; McAfee 1993; Hendry 1994) and its detailed analysis may help addressing the Scapa system which proved problematic as indicated by the range of proposed models.

During the late Early Hauterivian (S10 interval), reworked terrestrial and shelfal sediments of multi-source origin were transported via persistent multiple feeders across the fault-bounded, conglomerate-lined Halibut Shelf into the shallow Scapa halfgraben ("syncline") during sea-level rise. Sediments were further funnelled into the basin by a broad, shallow distributary system leading to renewed, basin-wide sand progradation in the central graben area where the bulk of the sand-grade material was deposited in sheet-like lobe and fringe

deposits. Distinct fan geometry and morphology are poorly established and a rather complex superimposition and lateral coalescence of lithofacies and fan components exists. The sediment accumulation pattern varies considerably spatially and temporally with an overall northward shift in depositional locus mainly driven by source area tectonism. Intrabasinal depressions captured turbiditic flows resulting in a locally confined, aggradational depositional style. Further complicating the depositional pattern are minor sediment contributions off the fault-scarp and/or directly off the shelf and/or the Claymore High complexly interfingering with the main turbidite system while the Claymore High represents a barrier on which turbidites onlap, pond or are axially deflected. Localised basin uplift resulted in erosion particularly in the southeastern and distal northern basin sectors.

In absence of an overall fan-shaped geometry and morphology, Riley *et al.* (1992) suggest to regard the individual “fan lobes” developing at the mouth of the different feeders as small fans which laterally coalesce. Laterally coalescing deposits (e.g. Miller Field: Garland *et al.* 1999), lack of distinct fan morphology and geometry and a highly variable facies distribution pattern (e.g. Brae turbidite system: Stow 1985b) are commonly interpreted to be indicative of slope apron systems, in this case akin to the faulted slope apron of Stow (1985a). However, Reading & Richards (1994) argue that slope aprons are largely fed by a line-source such as a slope/shelf where extensive slumping provides the bulk of the sediment in addition to a subordinate channel systems. The narrow, 200 - 700 m wide conglomeratic fringe lining the Halibut Shelf is frequently referred to as a conglomeratic apron (e.g. McAfee 1993; Hendry 1994; Oakman & Partington 1998) resulting from mechanical destruction of the faulted slope (McAfee 1993) rather than a conglomeratic hinterland source. Although the nature of the feeder system, shelf and the hinterland are largely unknown (Hendry 1994) this and previous studies suggest that mostly reworked shelfal sediment was funnelled into the basin via multiple, persistent and probably structurally fixed feeders (e.g. McAfee 1993; Hendry 1994) with minor input directly off the shelf edge, fault-scarp and the Claymore High. These multiple sources give rise to a less coherent system with disorganised sequences (Reading 1991) which is interfingering with the conglomeratic apron. Seismic data shows thickening of SSM deposits towards a basinal direction (McAfee 1993). Reading & Richards (1994) and Richards *et al.* (1998) classify systems fed by multiple feeders and sources as submarine ramp systems, giving it a broader application than the original definition of Heller & Dickinson (1985). The S10 interval exhibits characteristics of a sand/mud-rich and a sand-rich submarine ramp *sensu* Reading & Richards (1994). Their difference is based on notably different seismic representation and characteristic architectural elements if the net sand content is > 70%, however, they do acknowledge that boundaries between systems are essentially transitional. Although, the turbiditic sandstones are very clean (Hendry 1994), considerable shale accumulations are recorded throughout the S10 interval expressed as shale-rich fan fringe and interlobe/OVB deposits (enclosure 1). Mud/sand-rich submarine ramp systems are characterised by significant channel and levee but subordinate lobe formation (fig. 1.3). This pars with the depositional model Boote & Gustav (1987) and McAfee (1993) proposed for the SSM/SD interval respectively. However, the S10 interval appears to be dominated by geographically restricted little to non-channelized, sheet-like sandy deposits, i.e lobe, lobe fringe and fan fringe deposits, with subordinate, shallow channeling (*further discussion chapter 3.5.3*). The S10 thus appears to be more akin to a sandier member of the mud/sand-rich submarine ramp *sensu* Reading & Richards (1994), such as the modern Crati Fan (Ricci Lucchi *et al.* 1985) and the Quaternary Paola Basin (Trincardi *et al.* 1995), or a sand-rich submarine ramp such as the Montrose, Claymore-Galley and Tye Fields (*in* Reading & Richards 1994) and the Western Annot Sandstones (Sinclair 2000). The few observed overbank deposits (fig. 3.12), a feature of mud/sand-rich ramp systems, may possibly reflect source-driven fluctuating sand/mud content which led to their occasional formation when more shale was available to the system. Hendry (1994) suggested a sand-rich SSM submarine ramp model analogue to the Greenlandic Hareelv Formation, a “non-organised, line-sourced ramp-like slope apron to basinal turbidite system” (Surlyk 1978, 1987), the latter displaying characteristics of both ramp and slope apron systems. A clear separation of sand-rich slope apron and submarine ramp systems is regarded as sometimes problematic as they represent end-members of transitional systems (fig. 3.20). However, a line-source supplying the bulk of S10 sediment by slumping characterising slope apron systems is not envisaged for the S10, even as there is no recorded evidence for cut and fill channels just the indication of distinct, structurally fixed feeders zones funneling sediment into the basin during general sea level rise. Through a distributary system, sand is transported further into the relatively small basin leading to basin-floor deposition.

For simplification Reading & Richards (1994) purposely do not consider basin geometry and topography in any of their models which may substantially influence the sediment accumulation pattern and thus the shape and dimension of the specific architectural element.

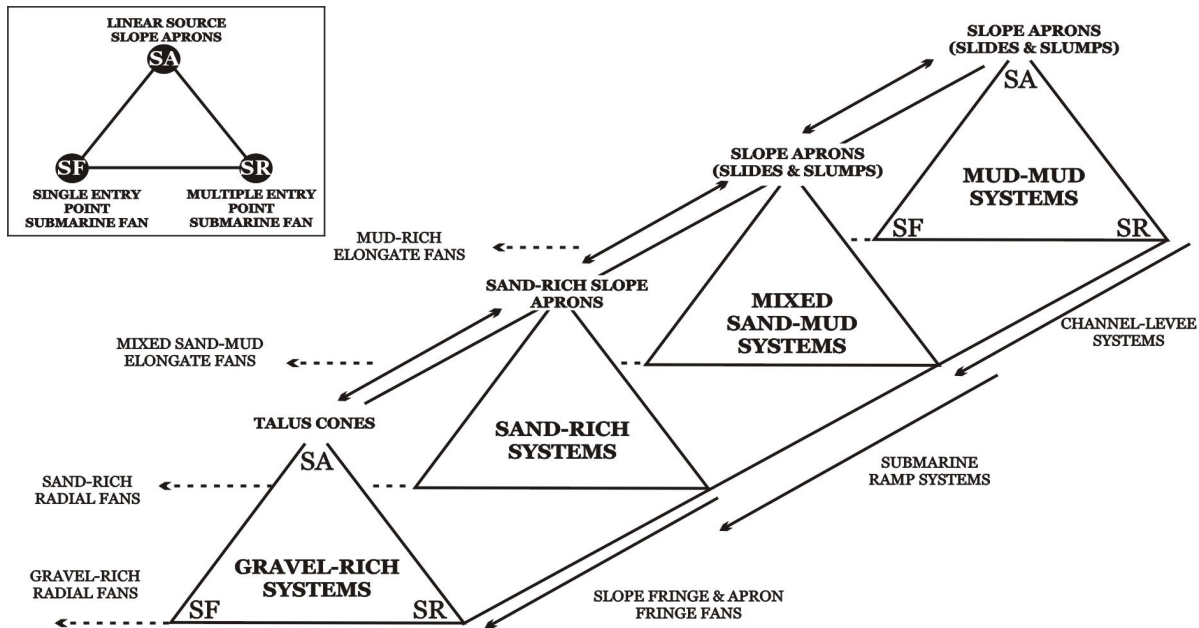


Figure 3.20: Classification of submarine-fans by (a) sediment supply mechanism, (b) dominant gain size and (c) number of entry points (from Richards *et al.* 1998).

Ultimately, the scale of observation plays an important role in the analysis of systems (Reading & Richards 1994). Riley *et al.* (1992) coalescing point-sourced “mini-fans” proves correct if only single feeders are considered, however, the (main) Scapa syncline appears to represent a multiple sourced mud/sand-rich to sand-rich submarine ramp-type system where the bulk of the sand is deposited in sandy little to non-channelized, laterally coalescing sediment bodies. A comprehensive analysis of the larger depositional system of the Scapa-Highlander Subbasin including the correlative, contemporaneous clastic deposits of the Highlander Field (Hendry 1994) and of the feeder system may yet yield a different perspective.

Many of the wells show overall fining-upward sequences indicating deepening conditions which is in accordance with the gradually rising sea level frequently described (Harker *et al.* 1987; Riley *et al.* 1992). However, some wells, notably well E1 in the central area remain distinctly coarse grained. This suggests other mechanisms than rising sea level to influence deposition. Harker *et al.* (1993) and Jeremiah (2000) consider tectonisms the most important control on sedimentation in the Outer Moray Firth, allowing, for example, the SSM system to develop an overall marl and shale depositional regime.

The depositional nature and the development of the S10 system appears to be fundamentally governed by tectonism. “Piano-key”-tectonism (*sensu* Stow 1985b) within the source area, uplifting different shelfal sectors at different times, effectively lowered sea level locally exposing poorly consolidated sediment to erosion/reworking through wave action and/or seismic events. Source area tectonism thus controlled the sediment supply to the basin and in combination with (older?) structural lineaments the pathways and thus the preferred geographic location of deposition within the basin (e.g. Miller Field: Garland *et al.* 1999). While the observed northward shift in time and activity of the feeders is a direct result of the shifting differential source area uplift, decreasing feeder activity probably follows denudation and subsiding source area tectonism.

Within the basin, the tectonic lineaments controlling the seafloor topography exerted the fundamental control on sediment accumulation resulting in the recorded aggradational, stacked pattern and elongate sandbody geometries. But flows captured by these intrabasinal depressions could due to the confinement become more erosional again akin to the accelerative flows of Kneller (1995) resulting in sediment transport further into the basin than under unconfined circumstances. Relocation of the fan axis resulted in repeated reconfiguration of the fan system as a consequence of either feeder channel switching, lobe offset, changing gradient and/or sediment flux.

Further complicating the sedimentary pattern are obstacle-forming debrites and slumps/slides off the different margins, resulting in deflection and/or ponding of turbidites (e.g. E3; well C15: Hendry 1994) The uplift and the intraformational erosion of VI deposits in the distal northern (E5Y) and eastern wells (21) will

most likely have contributed sediment to the active depositional areas. However, the nature of this probably unconsolidated, reworked sediment, the trigger of their remobilization and the transport and depositional process can only be speculated on.

Hydrodynamic sorting in the source area controlled the sedimentology and the nature of the largely turbiditic S10 system (Hendry 1994) which can lead to the accumulation of thick massive bodies particularly in restricted trough-basin fill complexes (Stow & Johansson 2000). Distinctly different overall grain sizes in closely adjacent wells 20/E7 suggest different sources of these.

Tectonism overriding rising sea level in controlling the nature of the S10 interval has frequently been observed in the North Sea (e.g. Brae turbidite system: Stow 1985b). Basin physiography and topography was been shown to fundamentally effect the shape of depositional elements as well as whole turbidite systems through progressive fault activity (e.g. Claymore Field: Kane *et al.* 2002), while topography can result in the preservation and/or erosion of sediments (e.g. VI subzone in wells E5Y/21).

Thus throughout the S10 interval tectonism enacted a fundamental control on sediment supply to the basin resulting in a phase of renewed sand progradation into the basin, as well as determining the location and shaping the overall geometry of the basinal deposits. The interplay of tectonism and sediment input thus fundamentally control the distribution of facies.

3.5.3 Lobe accumulation

Throughout the S10 interval, primarily non-channelized, sandy lobe deposits were accumulated. In proximal and distal positions lobe deposits appear to be channelized, i.e. associated with distributary channels, however, their association with lobe fringe / fan fringe deposits especially in the distal areas is more pronounced. The lobe deposits identified do not fit the classical lobe definition *sensu* Mutti & Normark (1987), their internal organisation, stacking pattern and geometry being strongly determined by shifting source area activity and confining seafloor topography.

The distinction of channelized and non-channelized sediments is not always easy. Also, complex relationships may exist between distributary channels and depositional lobes, when, for example, volumetrically large flows are not contained in the confines of a channel flow stripping leading to the development of “wing-like” sheet-sands outside of channel geometries, possibly developing into lobe-like bodies (e.g. CLTZ and proximal lobe zone of Cingöz Formation: *chapter 2.4.1*) which blurs the boundaries between these components. In outcrop these relationships may be relatively easy to establish - exposure permitting - however, when dealing with borehole data, this crucial lateral control is missing. In the subsurface, the identification of depositional environments relies heavily on the identification of facies associations and vertical sequences observed in a well. However, a comprehensive approach in subsurface analysis is essential, not only to determine the depositional environment and component associations, but also their temporal and spatial distribution, which requires the substantiation with seismic data.

The identification of lobes in the subsurface, its problems and limitations, are discussed in detail in chapter 5.

3.6 Conclusion

Previous studies have focused on analysing the diachronous SD reservoir unit, only the recently introduced more detailed biostratigraphic subdivision of the Scapa Sandstone Member enabled the reconstruction of zones VJ and VI, the so-called S10 interval.

- I) The S10 interval of the Scapa Sandstone Member appears to be akin to a multiple sourced mud/sand-rich to sand-rich submarine ramp system *sensu* Reading & Richards (1994) with some features of a slope apron system. Multiple feeder zones funnelling sediment off the Halibut Shelf and minor sources off the shelf, slope, Claymore High and intraformational sources give rise to a system with complex interdigitation of facies lacking clear proximal-distal trends. The S10 is dominated by sand lobe deposition and a subordinate distributary system, their location and geometry of sediment bodies are strongly determined by source-area and basinal tectonism.

- II) The S10 interval records renewed deep-water clastic progradation into the central Scapa Field area in an area which was previously dominated by shale-rich fan fringe (?) and basin-shale (?) S9 deposition. Internally, a distinct northward shift of sandy deposition occurs through zones VJ to VI.
- III) Although the S10 interval was deposited during gradually rising sea level, tectonism appears to be the fundamental control on the depositional nature and development of the S10 overriding sea level fluctuations. Lateral migration and local retrogradation of the system is in response to locally decreasing sediment supply and shifting sources caused by differential uplift of the source area. Source area tectonism controlled local sea level, the sediment volume and pathways into the Scapa syncline and thus the geographic location. Basinal tectonism resulted in probably fault-controlled intrabasinal depressions which captured flows resulting in thick aggradational patterns and localised, confined sediment accumulation.
- IV) Uplift in the eastern and distal northeastern area (21, E5Y) probably lead to intraformational erosion of zone VI.
- V) The bulk of the sand deposition took place in little to non-channelized, sheet-like lobe and lobe fringe deposits *sensu* Mutti & Normark (1987), however, their appearance is disparate to classical lobes. Sediment bypass close to the conglomeratic fringe resulted in detached lobes developing basinward from the base-of-slope. The shifting activity of the various feeder zones combined with a complex basinfloor topography resulted in localised, stacked, aggradational lobe accumulation of elongate geometry indicating that deposition was not altogether free to move. Individual lobes are mainly composed of sand high-density turbidites and diluted flows and possibly sandy debris flows *sensu* Shanmugam (1996).

3.7 Further work

In order to gain a more complete picture of the development of the S10 interval and the Scapa Sandstone Member (SSM) and thus the factors governing lobe accumulation in small, fault-controlled basins, further studies would benefit from:

- I) refined biostratigraphy of some of the already analysed wells to fully include and refine the existing as well as the inclusion of the other Main Scapa wells to verify and extend the S10 depositional model.
- II) extension of the present environmental and depositional model of the S10 interval for the whole SSM to examine larger spatial and temporal changes within the Scapa system including their controls.
- III) inclusion of profile desanding and tuff-stratigraphy for the S10 / SSM in aid of further, possibly more detailed interwell correlation.
- IV) inclusion of seismic data to gain more information about the nature of the feeder system (more stable due to incision?) as well as potential fault-scarp related topography within the actual syncline which may profoundly control the sediment accumulation pattern.

3.8 Summary

The S10 interval of the Scapa Sandstone Member forms part of the Lower Cretaceous infill of the Scapa Syncline in the north western Witch Ground Graben. During this time, a maximum of 236 ft (72 m) of sandstones, conglomerates and marls of early Valanginian to intra-late Hauterivian in age accumulated. The S10 interval records renewed clastic progradation into the central basin during a period of overall rising sea level. Localised source area uplift freed large volumes of sediments from the Halibut Shelf to the south

which were transported via turbiditic and sandy debris flows through fixed feeders across the fault-bounded, conglomerate-lined shelf into the narrow deep SE-NW trending syncline.

Sediments were further funnelled into the basin by a broad, shallow distributary system where the bulk of the sand-grade material was deposited in sheet-like lobe and fringe deposits. Distinct fan geometry and morphology are poorly established and a rather complex superimposition and lateral coalescence of lithofacies and fan components exists. The sediment accumulation pattern varies considerably spatially and temporally with an overall northward shift in depositional locus. Intrabasinal depressions captured turbiditic flows resulting in a locally confined, aggradational depositional style. Minor sediment contributions off the fault-scarp and/or directly off the shelf and/or the Claymore High complexly interfingering with the main turbidite system while the Claymore High represents a barrier on which turbidites onlap, pond or are axially deflected. Lateral migration and local retrogradation of the system is in response to locally decreasing sediment supply and shifting sources caused by differential uplift of the source area while intrabasinal tectonism resulted in localised erosion and sediment-remobilisation.

The S10 interval is best represented by the sand/mud-rich to sand-rich submarine ramp system *sensu* Reading & Richards (1994).

4 RESERVOIR CHARACTERISATION

As most sands in almost all submarine fan environments are originally porous and permeable, sandy depositional lobes *sensu* Mutti & Normark (1987) and related sheet-like sandy deposits provide excellent reservoirs if contiguous with adequate source beds (e.g. Normark *et al.* 1983; Richards & Bowman 1998). They are of great areal extent, tend to have a low percentage of total intergranular matrix and probably have some of the highest initial porosity (28 - 35 %) and permeability (200 - 4000 md) (McLean 1981; Risch *et al.* 1996).

Lobe and related sheet-like deposits do not form homogeneous reservoirs as different studies have shown (e.g. Schuppers 1995; Garland *et al.* 1999). Shales occurring at various scales within reservoirs constitute important barriers or baffles to fluid flow. Thus, for successful reservoir characterisation and hydrocarbon production, it is imperative to possess a detailed knowledge of the distribution of reservoir rocks and especially of their heterogeneities as well as their vertical and lateral geological variations. Much of the lobe character ultimately depends on the availability of sand and shale to a system. A combination of complex processes such as frequency of flow, composition, erosion, burial, compaction and diagenesis that occurred over millions of years fundamentally affect the reservoir, while, in particular, basin floor topography enacts one of the basic controls shaping lobe geometry and stacking pattern (e.g. Reading & Richards 1994).

The qualification of the geological variation of lobe deposits is typically undertaken at different scales, for example, the 3 scales of Mijnsen *et al.* (1993):

- i) *large-scale* variation between genetic units, for example lobes, is mainly concerned with geometries and internal configuration of sedimentary environments
- ii) *medium-scale* variation within genetic units is concerned with geometries and internal configuration of genetic units (e.g. width/depth ratios of genetic units, and sizes of baffles to flow).
- iii) *small-scale* variation due to compositional feature of the rocks is concerned with variation in rock properties caused by texture and composition of rocks, mainly porosity and permeability trends. Cementation and matrix content, for example, play an important role in reservoir reduction. The behaviour of density currents depositing turbidites can impart textural variations and sedimentary structures which contributed to permeability heterogeneity at probe permeameter, core plug and bed-scale.

Each reservoir scale is characterised by specific, intrinsic heterogeneities (Weber 1986). Hydrocarbon recovery greatly depends on good connectivity and interconnectedness, especially in thin reservoirs (Guerillot *et al.* (1992) and thus the classification and quantification of reservoir heterogeneities plays an important role in the quality of production forecast. The scale and orientation of shales as i) boundary shales (the surfaces between zones), ii) intrazone shales (heterogeneities within the zone) and iii) permeable/non-permeable lithotypes form the most important heterogeneities (e.g. Geehan & Underwood 1993).